Deconstructing Atlantic Intertropical Convergence Zone variability: Influence of the local cross-equatorial sea surface temperature gradient and remote forcing from the eastern equatorial Pacific

John C. H. Chiang,[1,2] Yochanan Kushnir, and Alessandra Giannini[3]

Lamont-Doherty Earth Observatory of Columbia University, Palisades, New York, USA

[1]   We investigate causes of interannual variability in Atlantic Intertropical Convergence Zone (ITCZ) convection using a monthly mean global precipitation data set spanning 1979–1999. Starting from the hypothesis of two dominant influences on the ITCZ, namely, the cross-equatorial gradient in tropical Atlantic sea surface temperature (SST) and the anomalous Walker circulation due to the rearrangement of tropical Pacific convection associated with the El Niño–Southern Oscillation, we analyze anomaly composites over the 1979–1999 period that best isolate the effects of each mechanism. Our results suggest that to first order, a strong anomalous Walker circulation suppresses precipitation over the tropical Atlantic, whereas an anomalous warm north/cool south SST gradient shifts the meridional location of maximum ITCZ convection anomalously north. We examined the processes underlying each of the two mechanisms. For the anomalous Walker circulation we find consistency with the idea of suppression of convection through warming of the tropical troposphere brought about by anomalous convective heating in the eastern equatorial Pacific. For the SST gradient mechanism our results confirm previous studies that link convection to cross-equatorial winds forced by meridional SST gradients. We find that positive surface flux feedback brought about through the cross-equatorial winds is weak and confined to the deep tropics. On the basis of the results of this and other studies we propose an expanded physical picture that explains key features of Atlantic ITCZ variability, including its seasonal preference, its sensitivity to small anomalous SST gradients, and its role in the context of tropical Atlantic SST gradient variability.   *INDEX TERMS:* 4215 Oceanography: General: Climate and interannual variability (3309), 3339 Meteorology and Atmospheric Dynamics: Ocean/atmosphere interactions (0312, 4504), 3354 Meteorology and Atmospheric Dynamics: Precipitation (1854), 3374 Meteorology and Atmospheric Dynamics: Tropical meteorology, 4522 Oceanography: Physical: Ocean Optics; *KEYWORDS:* Tropical Atlantic, precipitation, climate variability, El Niño–Southern Oscillation, Ocean-atmosphere interaction

1. Introduction

[2]   The Atlantic Intertropical Convergence Zone (ITCZ) is a narrow region usually located several degrees north of the equator that demarcates the transition from the southeast to the northeast Atlantic trades. The Atlantic ITCZ is associated with an organized zonal band of high precipitation that occurs predominantly over the ocean basin extending from the east coast of South America to the west coast of Africa. The convection has particular temporal and spatial characteristics. Its seasonal north-south migration lags the land-based ITCZ convection by roughly a quarter cycle, so that its northernmost extent occurs in boreal fall and its southernmost extent occurs in boreal spring [*Waliser and Gautier*, 1993]. It has a pronounced north-south asymmetry, occupying the Northern Hemisphere most months of the year except for boreal spring when it reaches the equator and extends into the Southern Hemisphere. Because of the close association between convection and the ITCZ we refer to the convection as ITCZ convection or, more simply, as the ITCZ.

[3]   The Atlantic ITCZ convection is unambiguously linked to precipitation over neighboring continents, especially northeastern Brazil and the Sahel and Gulf of Guinea coastal regions of West Africa, where interannual and interdecadal variations in precipitation result in prolonged intervals of drought and consequent economic hardship [*Hastenrath and Heller*, 1977]. The strongest interannual variability of the Atlantic ITCZ occurs in boreal winter and spring, when the ITCZ is at the southernmost extent of its annual migration and manifests itself primarily as a meridional displacement from its mean position during that time [*Hastenrath and Heller*, 1977; *Nobre and Shukla*, 1996]. In the other seasons the variability is not nearly as pronounced.

[4]   This ITCZ variability is associated with a leading statistical pattern of variability in tropical Atlantic sea surface temperature (SST) and winds [*Nobre and Shukla*, 1996]. The SST anomaly pattern is characterized by variations in two regions: one encompassing the northern tropical Atlantic basin from 5°N to 25°N and the other encompassing the southern tropical Atlantic basin from the equator to 25°S, such as to produce a gradient in the SST anomaly just north of the equator (around 2°–3°N). Associated

---

[1]Now at Joint Institute for the Atmosphere and the Ocean, University of Washington, Seattle, Washington, USA.
[2]Also at Department of Geography, University of California, Berkeley, California, USA.
[3]Now at National Center for Atmospheric Research, Advanced Study Program, Boulder, Colorado, USA.

with this gradient are cross-equatorial wind anomalies directed from the relatively cooler hemisphere to the warmer hemisphere. A warm north/cool south SST anomaly configuration, combined with a northward directed anomalous cross-equatorial flow, implies an anomalously northward displacement in the ITCZ. In this paper, we refer to this SST-wind-precipitation pattern as the tropical Atlantic gradient (TAG) pattern.

[5] From a climate dynamics viewpoint this pattern is important because the apparent links between SST, convection, and surface winds are quite distinct from those found in the tropical Pacific, namely, the El Niño–Southern Oscillation (ENSO) pattern, which arises from tropical air-sea interaction [*Bjerknes*, 1969]. *Hastenrath and Greischar* [1993] (hereinafter referred to as HG93) proposed a mechanism for this tropical Atlantic linkage between SST, convection, and surface winds by which the meridional gradient in anomalous SST generates anomalous cross-equatorial surface winds through the hydrostatic effect of SST on sea level pressure [*Lindzen and Nigam*, 1987]. The anomalous cross-equatorial wind is assumed to influence the position of convection, and this causal linkage has been supported in subsequent observational [e.g., *Ruiz-Barradas et al.*, 2000] and atmospheric general circulation model (AGCM) studies [e.g., *Chang et al.*, 2000; *Okumura et al.*, 2001]. *Nobre and Shukla* [1996] (hereinafter referred to as NS96) show that variation in trade wind strength precedes the development of basin-wide SST anomalies in boreal spring over the tropical Atlantic, thus providing evidence for the atmospheric origin of the SST anomalies. They show that the anomalous atmospheric patterns are phase locked to the seasonal cycle, peaking in the March-April-May season. Furthermore, they show evidence for El Niño–Southern Oscillation influence on Atlantic ITCZ position through a midlatitude "atmospheric bridge" [*Lau and Nath*, 1996] resembling the Pacific-North American (PNA) teleconnection pattern [*Horel and Wallace*, 1981] that affects SST over the northern tropical Atlantic. Thus NS96 proposed that ENSO works through the SST gradient mechanism to affect the Atlantic ITCZ. The influence of ENSO on the northern tropical Atlantic SST is well supported in other studies [*Curtis and Hastenrath*, 1995; *Enfield and Mayer*, 1997; *Klein et al.*, 1999; *Giannini et al.*, 2000]; in particular, Enfield and Mayer state that 50–80% of the northern tropical Atlantic SST variability is explained by ENSO. A recent investigation by *Hastenrath* [2000] focusing on the midlatitude atmospheric bridge supports the framework proposed by NS96 for ENSO influence on the Atlantic ITCZ through the PNA influence on the northern tropical Atlantic SST.

[6] The influence of ENSO on the tropical Atlantic via the midlatitude atmospheric bridge has recently been contrasted with an anomalous Walker circulation influence set up through the rearrangement of convection in the eastern equatorial Pacific. *Saravanan and Chang* [2000] argue from an AGCM study that the Pacific influence on the model tropical Atlantic climate is mediated through an anomalous Walker circulation, and *Chiang et al.* [2000] also argue from observations of global precipitation and other climate variables for a direct Walker circulation influence on the Atlantic ITCZ. The details of this influence are not well understood, although it is common to associate the Walker circulation with suppression of remote convection through subsidence caused by the descending branch of the direct circulation [e.g., *Kumar et al.*, 1999; *Goddard and Graham*, 1999].

[7] This observational study extends the earlier observational studies by HG93 and NS96 on the nature of Atlantic ITCZ variability. We assume that the anomalous Walker circulation and the local meridional SST gradient are the two dominant influences on boreal spring Atlantic ITCZ variability on interannual timescales. In our interpretation the meridional SST gradient incorporates not only locally generated variability but also all

midlatitude atmospheric bridge effects of ENSO on the Atlantic ITCZ (see the next paragraph). We exclude the influence of the Atlantic Niño [*Zebiak*, 1993] from our analysis since that influence is distinctly different from a physical standpoint and known to impact the boreal summer and fall climate rather than the spring [*Wagner and Da Silva*, 1994; *Chang et al.*, 2000; *Sutton et al.*, 2000]. The primary difficulty of separating out the response of the ITCZ to each of the mechanisms from observations lies with the fact that the strength of both covary with ENSO; the SST gradient does so partly (through ENSO influence on the north tropical Atlantic SST), and the Walker circulation does so almost fully [*Dai and Wigley*, 2000]. Thus the form of the decomposition is crucial to any observational analysis of Atlantic ITCZ variability; the form we take (see section 2.3) distinguishes our approach from previous studies, in particular the approach taken by NS96.

[8] Another assumption we make in our study, this time with regards to the ENSO influence on the Atlantic, is that the PNA-mediated (as opposed to the Walker circulation) influence on the Atlantic ITCZ works solely through its influence on the local meridional SST gradient (so that the PNA-mediated ENSO influence contributes to part of the total meridional SST gradient variability). In particular, we assume no PNA-mediated direct atmospheric influence of ENSO on the Atlantic ITCZ. We think that this is a good assumption given the results of NS96 and also the more recent analysis by *Hastenrath* [2000] and that the strongest PNA influence occurs several months prior to the maximum Atlantic ITCZ variability in boreal spring, implying the need for an intermediate step (the north tropical Atlantic surface ocean) to explain the time lag. We will show later on that our composite results are consistent with this assumption, but we caution the reader to be aware of our working assumptions.

[9] Focusing on the ITCZ as the yardstick of Atlantic climate variability offers a perspective on tropical Atlantic climate change that differs from the usual focus on SST and surface winds. Precipitation reflects in a statistically averaged sense the surrounding climatic conditions and offers a distinct advantage when investigating the relative influence of remote and local forcing. Since convection is a response to vertical instability, it depends both on upper troposphere and near-surface conditions, and so both remote influences (more strongly felt above the boundary layer) and local influence (felt most strongly at the surface) are likely to play significant competing roles. There are drawbacks to using precipitation as the analysis field, however; it is much noisier, and observational data sets over the oceans are significantly shorter in duration compared with available SST and wind data sets (typically only from 1979 to present).

[10] Understanding convection is necessary in order to understand ocean-atmosphere interactions in the Atlantic. The impact of convection in the context of the TAG have only been implicitly investigated and usually through statistical linkage between SST and winds. This neglect is surprising because convection is a major component of the tropical atmospheric circulation, converting the convectively available potential energy into energy of motion and heat. It is thought to be an integral part of the ENSO mechanism through its effect on the Walker circulation: the strengthening and westward displacement of convection cause stronger zonal surface winds that pile up more surface waters to the west. The point is that change in the ITCZ is likely to impact the tropical Atlantic Ocean through its effects on surface winds (and possibly also through the surface radiative balance) and conceivably results in positive feedback between the tropical Atlantic Ocean and atmosphere.

[11] Our study is arranged in two major parts. In section 2 we present the results of an observational study of the Atlantic ITCZ variability that takes both the anomalous Walker circulation and SST gradient influences into account and attempt to isolate each
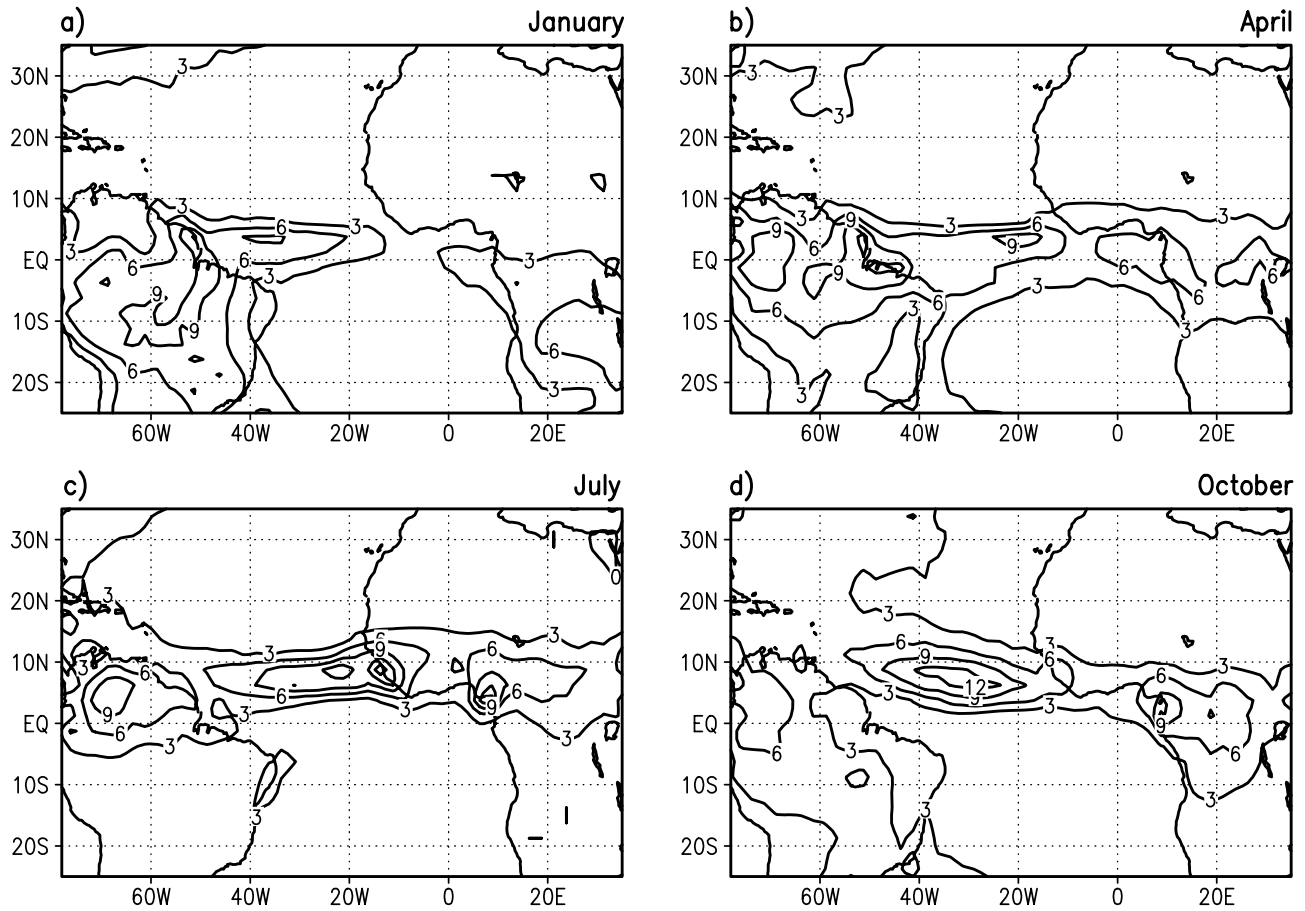
Figure 1.   Observed climatology of precipitation over the tropical Atlantic for (a) January, (b) April, (c) July, and (d) October. The contour interval is 3 mm/d.

mechanism through a suitable decomposition. Hereinafter we refer to the two mechanisms (influences) as the Walker and gradient mechanisms (influences). We take advantage of recent satellite estimates of precipitation and a corresponding data set of SST and surface winds to derive a complete characterization of how the ITCZ, SST, and near-surface winds vary as a result of each of the two mechanisms. Following NS96 and other studies [e.g., *Enfield and Mayer*, 1997; *Chang et al.*, 2000; *Sutton et al.*, 2000] we assume that seasonality is an important component of tropical Atlantic climate variability. Consequently, we examine the evolution of the ITCZ and associated climate behavior from its beginnings in the September prior to the peak variability seasons of boreal winter and spring through the following August. The added benefit of such a time-dependent analysis is that cause and effect may be distinguished, which is important to understanding the relationship between the winds, SST, and precipitation.

[12]   In section 3 we take advantage of the observational results, as well as results of other observational and theoretical studies, to examine the mechanisms underlying each of the two influences on the ITCZ and the background conditions that make the ITCZ susceptible to these mechanisms. In particular, for the gradient mechanism we extend the dynamical explanation of HG93 to form an expanded physical picture that explains the characteristic features of boreal spring Atlantic ITCZ variability.

[13]   Before we begin, we offer a word of caution to the reader. Because of the relatively short length (21 years) of available ocean precipitation data, we cannot establish the level of statistical confidence in our results that we would like. We therefore consider

our study to be exploratory rather than final. In lieu of statistical confidence, we appeal to related observed fields (surface winds and SST in particular) and current understanding of tropical ocean-atmosphere dynamics to demonstrate the reasonableness of our results and analyses.

2.   Observational Analysis

2.1.   Data

[14]   We use the merged satellite and rain gauge data set of *Xie and Arkin* [1997], which is global on a 2.5° by 2.5° longitude/latitude grid and reports monthly mean precipitation. We take the data from January 1979 to August 1999. Atmospheric and surface fields between September 1978 and August 1999 are taken from the National Center for Atmospheric Research/National Centers for Environmental Prediction (NCAR-NCEP) reanalysis data set [*Kalnay et al.*, 1996], which reports global monthly means on a ~1.875° by ~1.875° longitude/latitude grid.

2.2.   Atlantic ITCZ Position and Magnitude

[15]   Figure 1 shows the monthly climatological ITCZ, the band of maximum precipitation over the tropical Atlantic between 10°S and 20°N, extending from the east coast of South America to the west coast of Africa, for January, April, July, and October. Despite some noticeable zonal asymmetry in its spatial distribution, the oceanic Atlantic ITCZ is clearly zonally symmetric to first order and migrates as a unit. We therefore use zonal averages of precipitation over the Atlantic basin from 35°W to 15°W to track the ITCZ in its seasonal migration. The
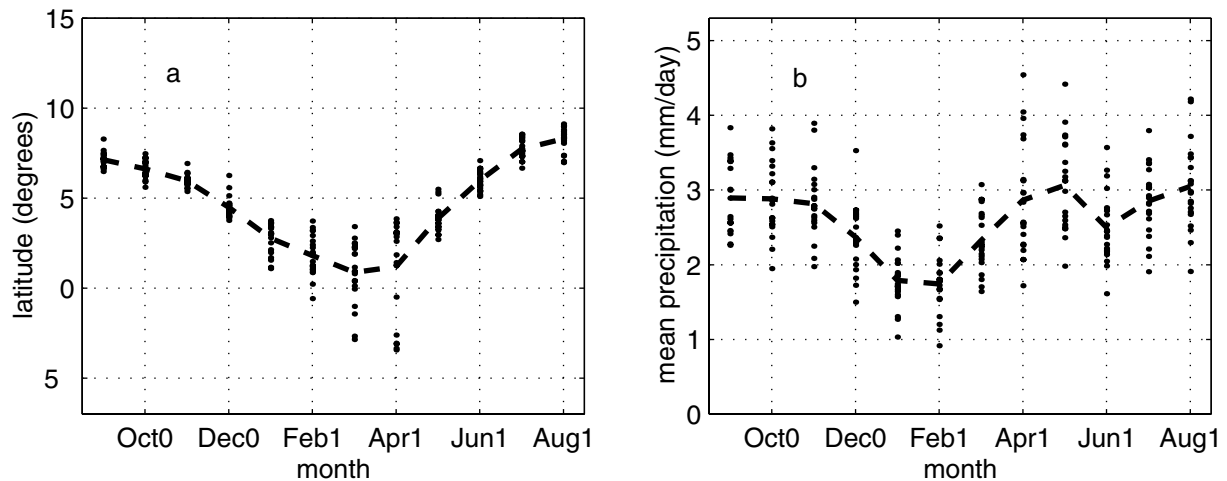
Figure 2. (a) The latitude position of maximum precipitation averaged between 35°W and 15°W for January 1979 to October 1999, plotted by month. (b) The latitude position of maximum precipitation averaged over 35°W–15°W and 15°S–20°N for January 1979 to October 1999, plotted by month. The dashed curves represent the mean position for the given month. The dots indicate values for individual years.

ITCZ clearly extends beyond 35°W and 15°W, but we restrict the range of longitudes averaged to avoid complications with convection over land. We define two summary statistics of this zonally averaged ITCZ that measure the position and magnitude, namely, the position of the precipitation maximum and precipitation averaged over the range of 15°S–20°N. The latitudinal position of maximum precipitation is found through a parabolic fit to the precipitation values at the grid point of maximum precipitation and at grid points immediately to the north and to the south of it. The asymmetric latitude range taken for the averaging is in keeping with the northern hemispheric preference of the Atlantic ITCZ.

[16] Figure 2a shows the variability in position of the Atlantic ITCZ during its evolution from September through to the following August by superimposing together data from all years in the rainfall data set. The ITCZ position migrates southward from its maximum northward position in August, reaching its southernmost point between February and April before migrating back up north. February, March, and April are also the months of maximum variability in position with the southernmost position ranging from 4°S to 4°N. The precipitation magnitude (Figure 2b) is fairly uniform at ∼2–3 mm/d in all months. Variability in the magnitude peaks in April and May, ranging from 1.7 to 4.5 mm/d.

[17] The position and magnitude are not independent measures of ITCZ variability: position and magnitude are significantly negatively correlated (at the 5% level using a two-sided t test) in January, April, May, and July (Figure 3a), so that there tends to be more rainfall if the ITCZ remains farther south during those months. There is persistence in the ITCZ position between December and January through June and July, except between March and April (Figure 3b); so, for example, if the ITCZ is anomalously southward in February, it is likely to be so in March. Finally, the precipitation magnitude also exhibits persistence between April and May, June and July, and July and August (Figure 3c); so, for example, if precipitation is high in April, it is likely to be so in May.

2.3. Indices for Decomposition

[18] We introduce two indices, the eastern equatorial Pacific (EEP) index and the TAG index (see sections 2.3.1 and 2.3.2), that capture the strength of the Walker and gradient mechanisms, respectively, for the purpose of choosing compo-

site years between 1979 and 1999 that best represent each influence.

2.3.1. EEP index for the Walker influence. [19] We use the EEP tropical heating index of *Chiang et al.* [2000] as a measure for the Walker circulation strength. This precipitation index is constructed by projecting rainfall amounts at each longitude on a meridionally varying Gaussian function centered on the equator with an e-folding distance of 1967 km. The profile follows the meridional structure of a Kelvin wave; the e-folding distance is derived assuming a vertical mode equivalent depth of 200 m, which is approximately the depth for the first baroclinic mode of the tropical atmosphere (we note that the shape of the index is insensitive to the chosen equivalent depth over the range 50–400 m). The resulting values from 180°W to 80°W, the longitudinal extent of the SST anomaly of El Niño events, are then summed to form the index. The assumptions behind the design of this index are as follows:

1. We assume that ENSO is the driving force for the shift in the Walker circulation [*Dai and Wigley*, 2000]; thus our index is based in the eastern equatorial Pacific.

2. The strength of the Walker circulation anomaly is more accurately measured by the strength of precipitation anomalies and not SST anomalies. *Chiang et al.* [2000] showed the strong and highly nonlinear relationship between SST and precipitation in the central and eastern equatorial Pacific (the Niño3 region, 5°S–5°N and 150°W–90°W), in particular, the disproportionate effects of El Niño on precipitation as opposed to La Niña.

3. The influence of eastern equatorial Pacific heating on the tropical Atlantic is best measured through the amplitude of precipitation symmetric about the equator. This is in keeping with *Gill*'s [1980] classic study, which indicates that equatorial Kelvin waves that communicate their influence from west to east are forced by symmetric heating about the equator.

[20] The striking feature of the index (Figure 4a) is the asymmetry in response between El Niño and La Niña conditions: strong El Niños are characterized by a pronounced increase in precipitation, whereas the drop in precipitation during La Niña years is not nearly as pronounced. This observation motivates us to distinguish the high-precipitation years (1982–1983, 1986–1987, 1991–1992, and 1997–1998, the Walker years) from the others to form a two-bin categorization (strong and weak) of the Walker
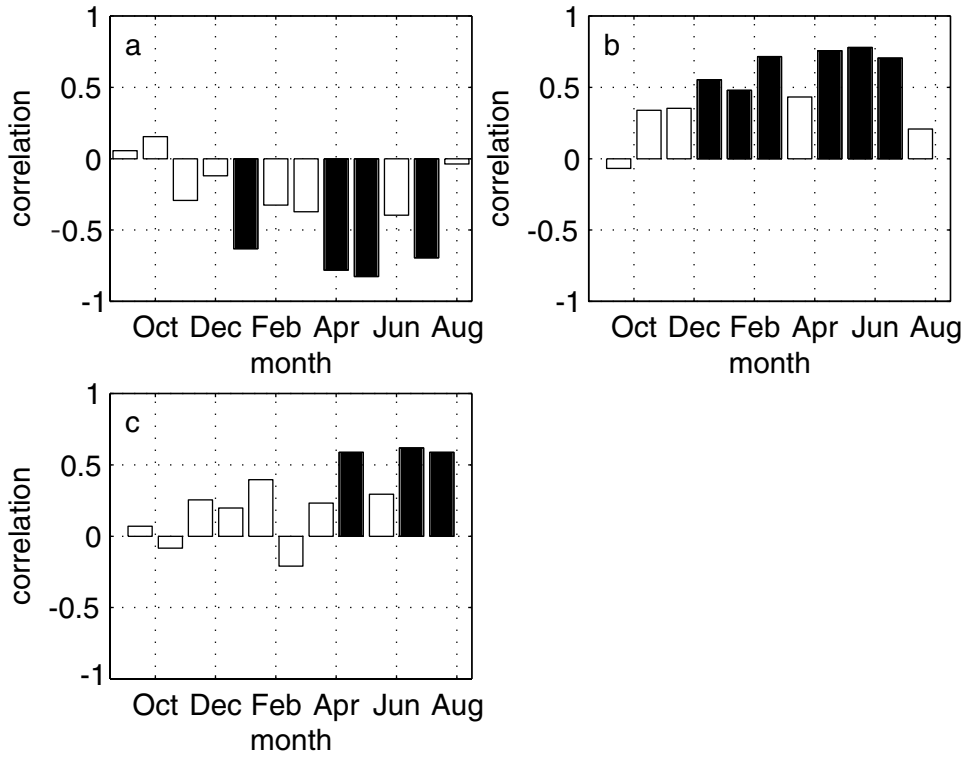
Figure 3. Rank correlation between (a) position of maximum Intertropical Convergence Zone (ITCZ) precipitation and magnitude, (b) position of maximum ITCZ precipitation in successive months, and (c) precipitation magnitudes in successive months. Solid bars represent correlation significant at the 5% level (using a two-sided t test). An intermediary bar between months implies the rank correlation taken between them.

influence. Note that we define our year to run from the previous September through the following August since we are interested in the events leading up to and beyond the boreal spring ITCZ response.

2.3.2. TAG index for the gradient influence. [21] Our index for the Atlantic cross-equatorial gradient (TAG index) is the difference between the northern tropical SST anomaly averaged over the Atlantic basin (east of 60°W) from 5° to 25°N and the
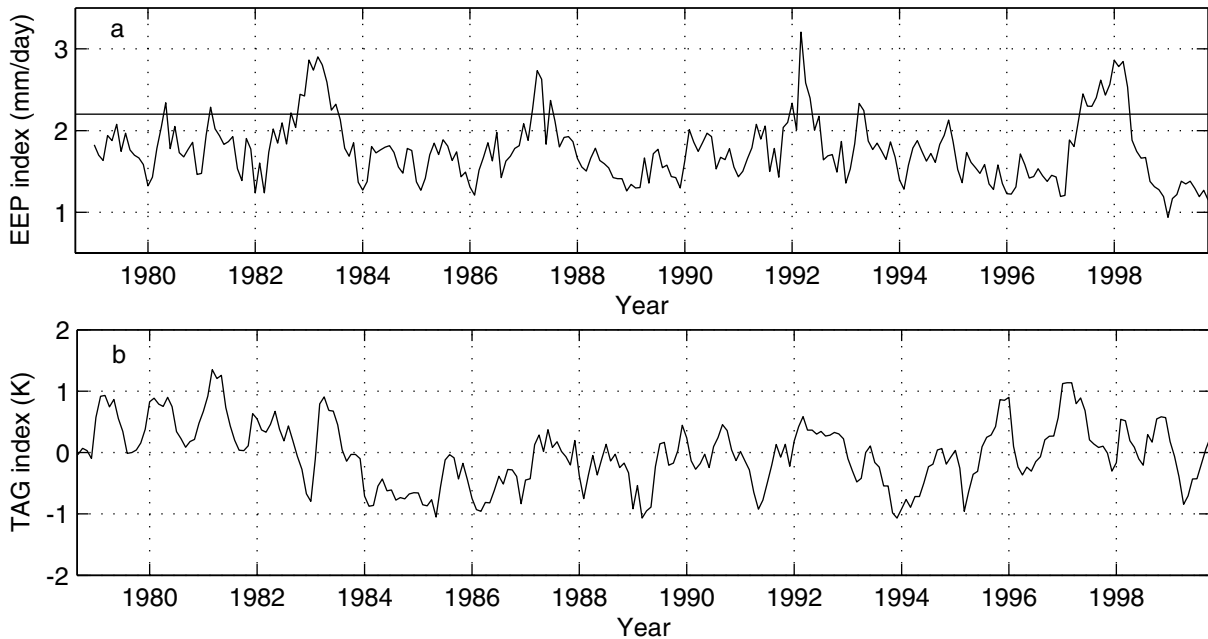

Figure 4. (a) The eastern equatorial Pacific (EEP) index for January 1979 to October 1999. The solid horizontal line at the EEP value just above 2 mm/d distinguishes between strong and weak years. (b) The tropical Atlantic gradient (TAG) index over the same period.
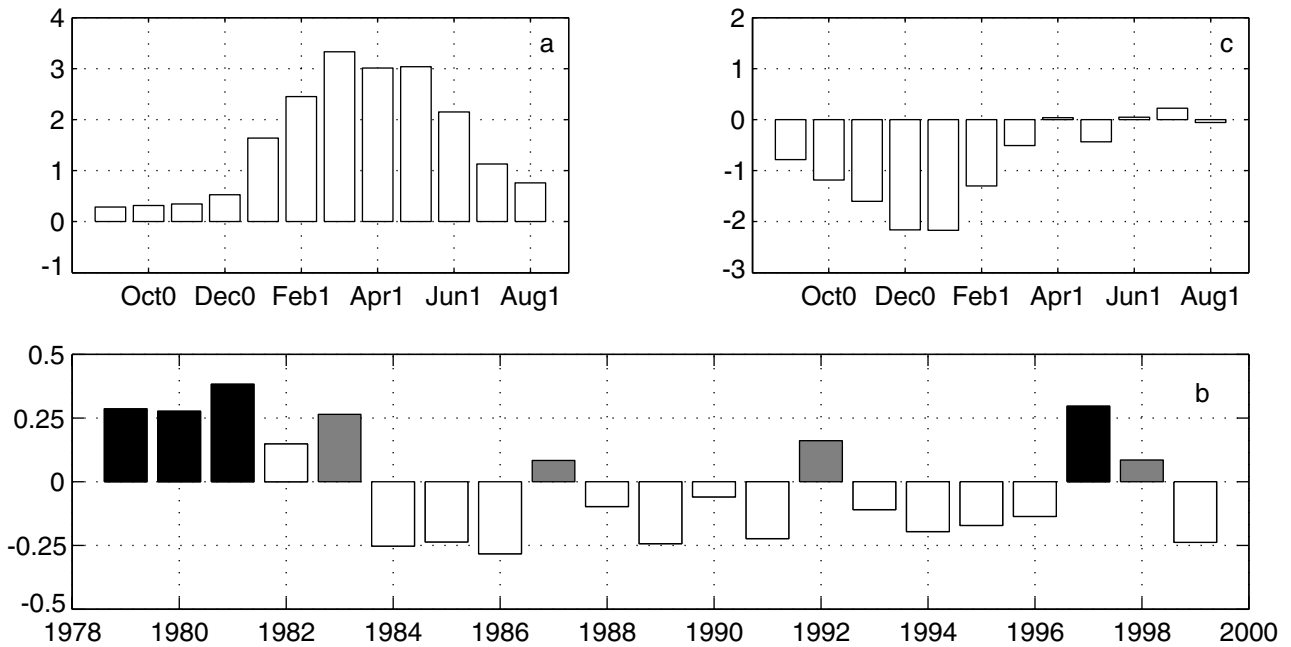
Figure 5. (a) The first rotated pattern of monthly amplitudes (empirical orthogonal function (EOF) 1) derived from an singular value decomposition (SVD) analysis of the TAG index and (b) the annual time series corresponding to the pattern of monthly amplitudes shown in Figure 5a (PC 1). Shaded, solid, and open bars are the Walker, gradient, and backgrounds years, respectively. (c) The second pattern of monthly amplitudes in the SVD analysis.

southern tropical SST anomaly averaged over the basin between 5° and 25°S (monthly time series shown in Figure 4b). We avoid the tropical belt from 5°S to 5°N because the dynamics determining SST over the equatorial region differ from that to the north and south of it.

[22] We want to find an interannual index that best represents the strength of the gradient influence. The values of the TAG index depend strongly on the season; they tend to be largest in the boreal spring. This is in some respects similar to the evolution of ENSO in the Pacific, which is also "locked" to the annual cycle. While the
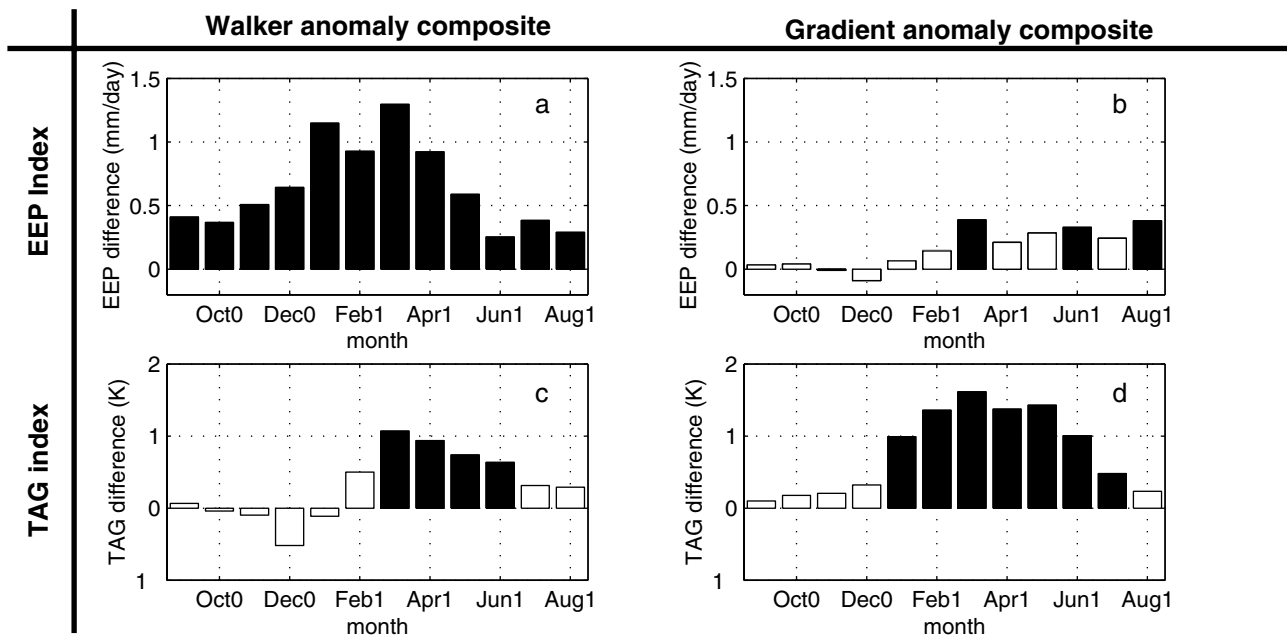

Figure 6. EEP and TAG values for the Walker and gradient anomaly composites. Solid bars indicate significance at the 5% level. (a) EEP values for the Walker anomaly composite. (b) EEP values for the gradient anomaly composite. (c) TAG values for the Walker anomaly composite. (d) TAG values for the gradient anomaly composite.
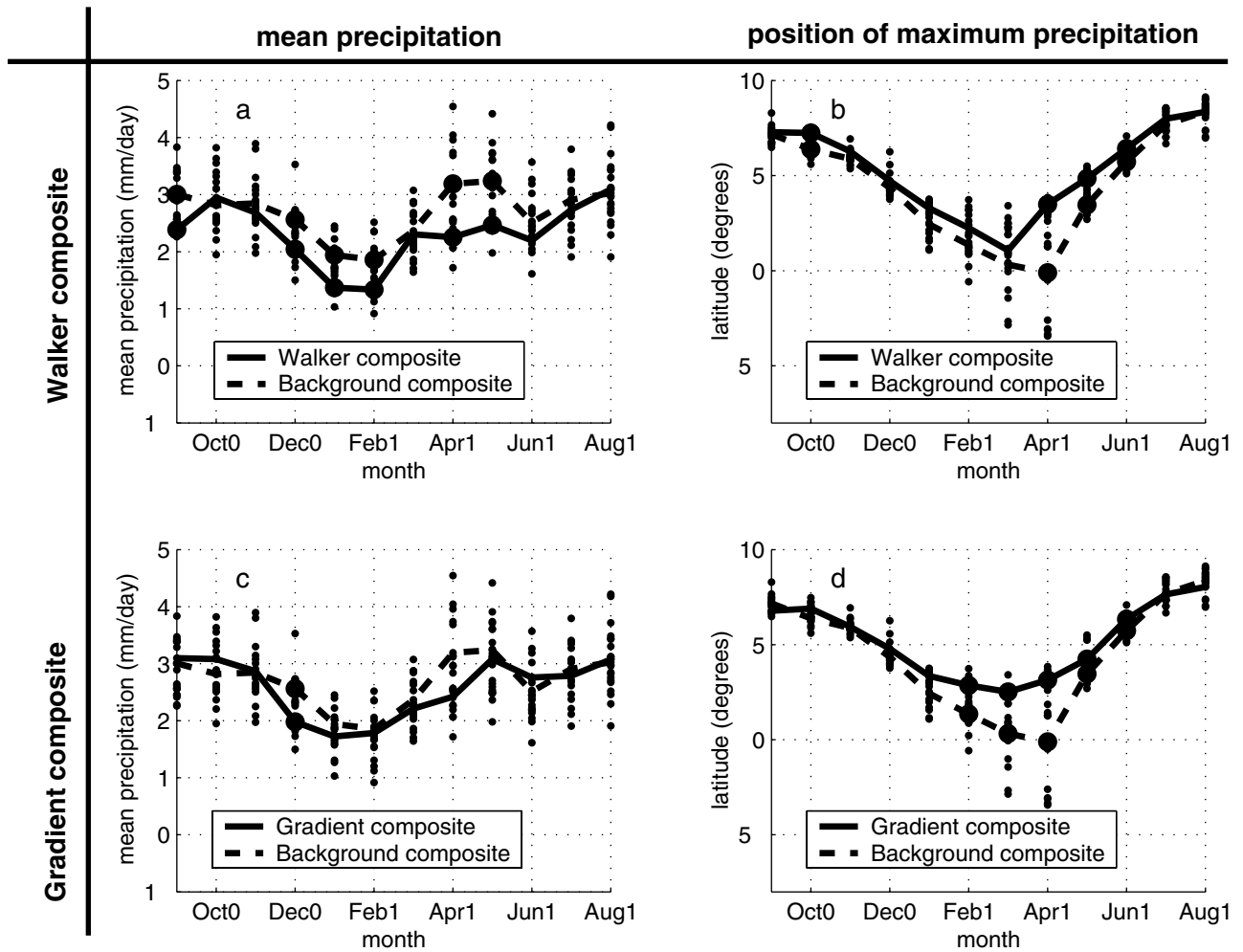
Figure 7. Walker and Gradient composites for position of maximum ITCZ rainfall and precipitation magnitudes. (a) Precipitation magnitude for background years (dashed line) and for Walker years (solid line). The large circles indicate the months where the difference in the means is significant at the 5% level. (b) Same as Figure 7a but for the latitudinal position of maximum precipitation. (c) Same as Figure 7a but for gradient years. (d) Same as Figure 7b but for gradient years.

reasons for such evolution in the tropical Atlantic are not clear a priori, we assert that interannual variability of the gradient follows a typical seasonal modulation. In order to extract the typical seasonal evolution we regroup the index time series into consecutive 12-month bins starting from the September of year 0 (Sep0) to the August of the following year, year 1 (Aug1). The data are then arranged into a matrix with 12 columns (one for every calendar month from Sep0 to Aug1) and 21 rows (1978–1979 to 1998–1999). Next, we apply a singular value decomposition (SVD) on the resulting matrix. The decomposition yields the principal components (PCs; 1 value per year) and empirical orthogonal functions (EOFs) (vectors of 12 weights, one for each calendar month) of the TAG time series. We then subject the two dominant PCs of the SVD to a varimax rotation [*Horel*, 1981]. We selected only the dominant two eigenvectors of the SVD for the rotation on the basis of *Preisendorfer*'s [1988] "rule N" test for significance under a white noise null hypothesis. The two rotated patterns of the TAG index are robust. The first two eigenvectors of the SVD prior to rotation are well separated from each other and also from the third eigenvector that explains 3.6% of the variance. A similar calculation but taken over a longer (1856–1999) SST data set [*Kaplan et al.*, 1998] shows that the first two rotated patterns remain essentially the same, explaining approximately the same amount of variance.

[23] The first rotated "weight" pattern (Figure 5a) shows a slowly evolving gradient anomaly peaking between January, year 1 (Jan1) and June, year 1 (Jun1) and possesses the same sign over the entire period from Sep0 to Aug1. This mode, explaining 65.3% of the total variance, represents the dominant SST gradient evolution peaking in boreal spring, and we use its corresponding times series (Figure 5b), hereinafter referred to as principal component 1 (PC1), as our interannual index for the gradient influence. We choose the four strongest positive (warm north/cool south) PC1 years (1978–1979, 1979–1980, 1980–1981, and 1996–1997) as our gradient years.

[24] Note that our approach differs from the way that NS96 chose their representative years for their composite analysis for the gradient influence: they chose their years on the basis of the time series of the first EOF of tropical Atlantic March-April-May SST anomalies, taken when the ITCZ displacement is most pronounced. Our reason for deriving the composite differently is that it is not clear whether the March-April-May SST gradient is a cause or a consequence of the ITCZ displacement. Because PC1 develops its gradient before the peak ITCZ displacement months, we avoid this ambiguity. However, it turns out that the years NS96 chose for the warm north/cool south gradient are exactly those years when our interannual gradient index (Figure 5b) is positive for the time period that their analysis years overlap with ours (1979–1987),
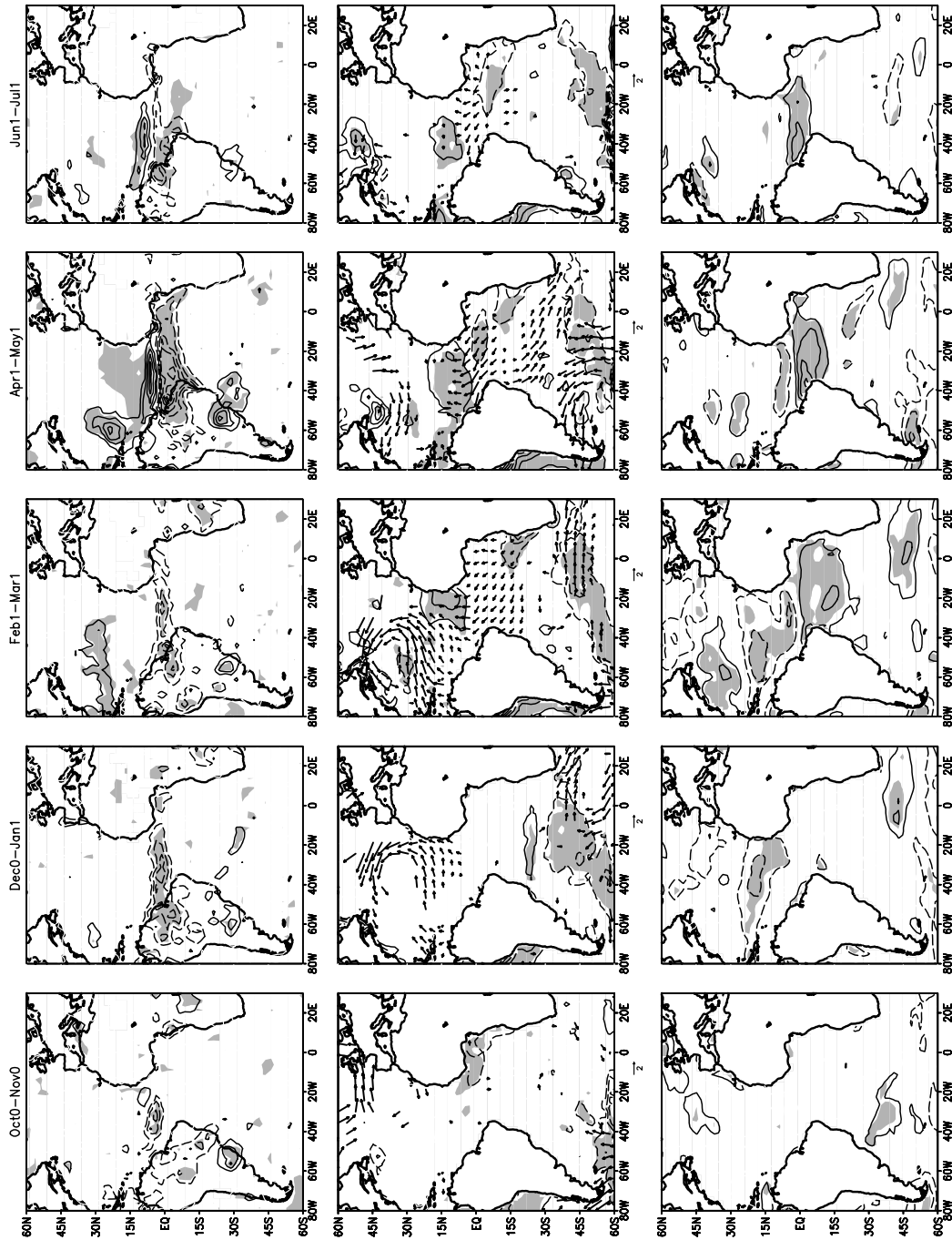
Figure 8. Walker anomaly composite maps. (top) Precipitation anomalies (contour interval 1 mm/d). Shaded regions indicate significance at the 5% level, and negative anomalies are dashed. (middle) Sea surface temperature (SST) anomalies (contour interval 0.5 K) and 10-m wind vectors (reference wind vector 2 m/s). Shaded regions indicate significance for SST differences at the 5% level, negative anomalies are dashed, and only wind vectors where either zonal or meridional wind is significant at the 10% level are plotted. (bottom) The 10-m wind speed anomalies (contour interval 0.5 m/s). Shaded regions indicate significance at the 5% level, and negative anomalies are dashed.

namely 1978–1979, 1979–1980, 1980–1981, 1981–1982, 1982–1983, and 1986–1987. However, our selection criteria lead us to bin 1982–1983 and 1986–1987 in our Walker composite (see section 2.3.3) and to not include 1981–1982 in the gradient composite, as the SST gradient associated with that year was comparatively small.

[25] How representative is pattern PC1 of the "typical" evolution of the SST gradient anomaly that affects boreal spring Atlantic ITCZ variability? We mentioned above that PC1 explains the majority (65.3%) of the total variance of the TAG index and that it peaks in boreal spring; so it is clear that PC1 is the best representative interannual time series for the gradient mechanism. The second rotated pattern (Figure 5c) also explains a significant (23.4%) fraction of the variance. However, the variations of its associated time series (PC2) occur in boreal winter (December, year 0 (Dec0) to Jan1) and have little bearing on boreal spring and early summer state of the gradient which are captured by PC1. It is the latter variations that are linked to the ITCZ variability addressed in this study, and those are described efficiently by PC1.

2.3.3. Composites. [26] All years for which we have precipitation data (1979–1999) are split into three groups according to the indices above: (1) Walker years 1982–1983, 1986–1987, 1991–1992, and 1997–1998; (2) gradient years 1978–1979, 1979–1980, 1980–1981, 1996–1997 (note that for 1978–1979 we do not have precipitation data from September 1978 to December 1978); and (3) background years all years excluding the gradient and Walker years. The difference between the mean of the Walker (gradient) years and the mean for the background years is our anomaly composite; hereinafter we refer to them as the Walker (gradient) anomaly composite, as opposed to the Walker (gradient) composite, which is simply the mean of the four Walker (gradient) years without the mean of the background years subtracted out. The Walker years together with the gradient years comprise all except one year in the 21-year record with a significant warm north/cool south gradient (Figure 5b). Hence the background years are basically the warm south/cool north years, and both the Walker and gradient anomaly composites are composites of positive TAG minus negative TAG index, except that in the Walker anomaly composite a strong Walker influence is also present. A valid criticism regarding this way of grouping the years is the coarse two-bin categorization for each forcing. A more complete grouping would be to define a three-bin categorization of "positive," "neutral," and "negative" years for each forcing, Walker or gradient. This grouping would have the advantage of showing nonlinearity in the response, in particular, to a positive or negative gradient influence. We are obviously limited by the length of the precipitation time series and cannot apply the more complete grouping approach.

[27] Figure 6 shows how much of each of the two influences appears in each composite. Figure 6a shows that the Walker mechanism is strong in the Walker anomaly composite: the EEP difference is positive for all months between Sep0 and Aug1 and peaks between Jan1 and April, year 1 (Apr1). A two-sample *t*test shows that the difference is significant at the 1% level for all months between November, year 0 (Nov0) and May, year 1 (May1), and also for Sep0; the other months are significant at the 5% level. By contrast, EEP values for the gradient anomaly composite (Figure 6b) show that the Walker mechanism essentially does not operate there.

[28] The gradient mechanism is strong in the gradient anomaly composite (Figure 6d): the TAG difference there is positive for all months between Sep0 and Aug1 and peaks between Jan1 and Jun1. The gradient mechanism is also significant in the Walker anomaly composite (Figure 6c): the TAG difference is positive from February, year 1 (Feb1) onward and is statistically significant at the 5% level between March, year 1 (Mar1) and

Jun1. The gradient influence starts earlier (Jan1) in the gradient anomaly composite as compared to the Walker anomaly composite (Mar1), and the magnitudes are approximately half as large in the Walker anomaly composites. Prior to Mar1 the gradient influence is not significant in the Walker anomaly composite, and this may be the time to extract the "pure" Walker influence in the data.

[29] Because the composites are not entirely successful in isolating each mechanism, we remind the reader to take care in distinguishing between the composite and the influence (mechanism) upon which they are based. We think the reason why we could not isolate each mechanism is because the EEP and TAG indices are not fully independent of each other; in particular, Walker years generally have positive TAG values (see Figures 6a and 6c). This likely occurs because ENSO contributes to both the Walker and gradient mechanisms. We further caution the reader not to view the gradient mechanism as originating solely from within the tropical Atlantic; as we have discussed earlier (see section 1), we assume that ENSO influences the gradient mechanism through the PNA. This is in addition to any other local or remote influences on the SST gradient.

2.4. Results With Walker and Gradient Influences Inferred From the ITCZ Time Series

2.4.1. Walker composite. [30] We examine the evolution of the Walker composites of ITCZ magnitude and position (Figure 7). The striking feature is suppression of the precipitation magnitude from Dec0 through May1 in the Walker years, with Mar1 being the exception (Figure 7a). The difference in the mean is significant at the 5% level over that period. The lack of a strong relationship in March between the Atlantic ITCZ and Pacific/Atlantic SST was also shown by *Uvo et al.* [1997] from analysis of a much longer data set: They showed that northeast Brazil rainfall during March, a good proxy for the Atlantic ITCZ at that month, was apparently not associated with any remote sea surface conditions.

[31] The migration of the ITCZ maximum position also has a particular feature: from November, year 1 (Nov1) through Mar1 the ITCZ behavior conforms to the norm (Figure 7b). In Apr1, however, the Walker ITCZ maximum suddenly favors an anomalously northward position. The anomalous northward position of the ITCZ in the Walker years persists through Jun1. Note that there is also a significant anomalous northward positioning of the ITCZ in October, year 0 (Oct0) but the difference in position is relatively small.

2.4.2. Gradient composite. [32] Figure 7c shows that the precipitation magnitude for the gradient years conforms to the mean of the background years except for Dec0 and possibly Apr1. The results for Dec0 and Apr1 are questionable because they occur in isolated months and, furthermore, the significance is barely at the 5% level for Dec0 and only at the 10% level for Apr1. The TAG effect on the position of the precipitation maximum is more convincing: Gradient years (Figure 7d) are characterized by an anomalously northward ITCZ position from Jan1 through Jun1, the significance level being 5% for Feb1 to Jun1 and 10% for Jan1.

2.5. Results With Walker and Gradient Influences on the Atlantic ITCZ Inferred From Anomaly Maps

2.5.1. Walker anomaly composite. [33] Figure 8 shows the evolution of anomalies in the Walker anomaly composite. For space reasons we show the evolution only at 2-month resolution from Oct0 to Nov0 and Jun1 to July, year 1 (Jul1), although in our following discussion we will describe some features of the evolution at monthly resolution. Significance is assessed through a two-sample *t* test, and shaded regions indicate significance at the
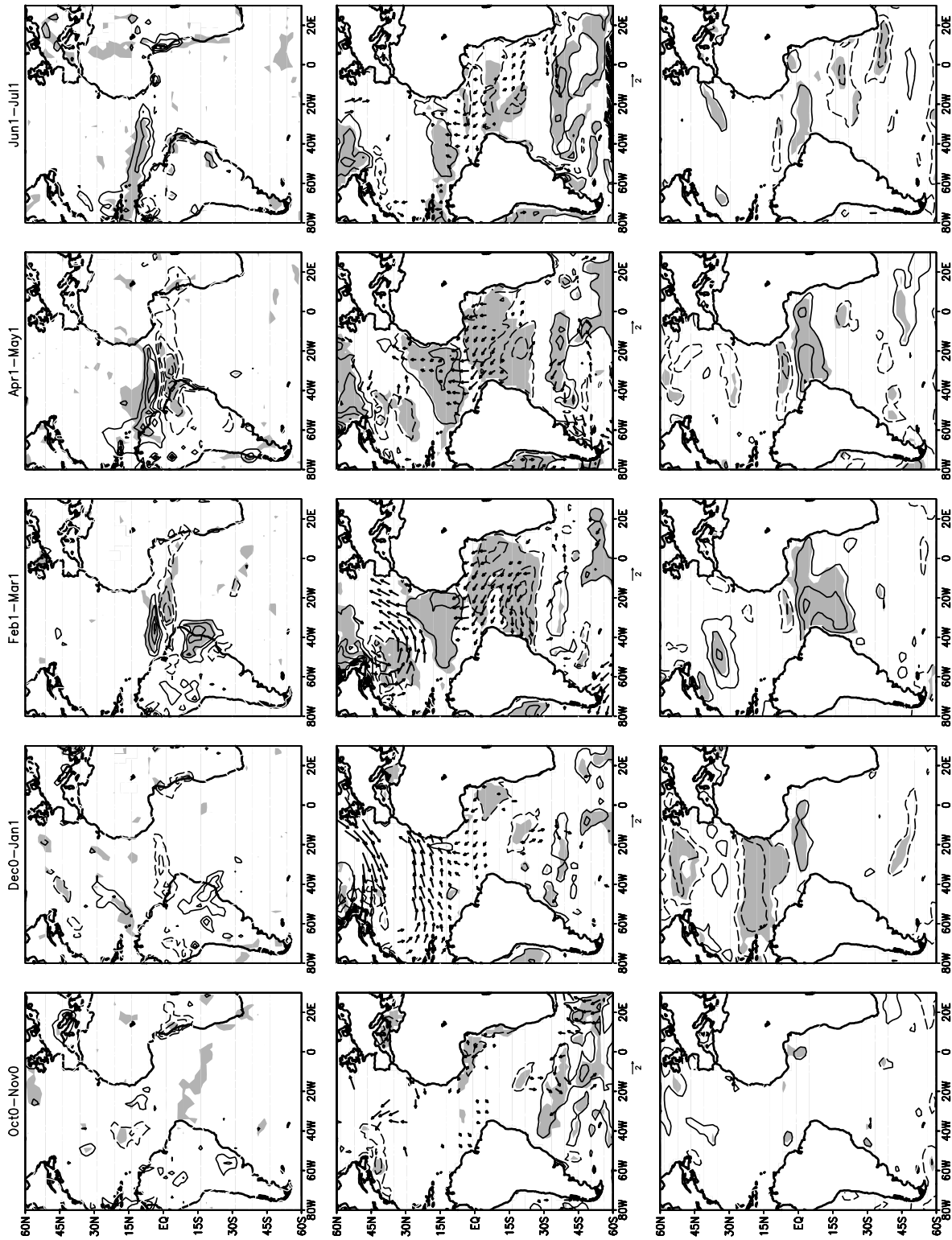
Figure 9.   Same as Figure 8 but for the gradient anomaly composite.

5% level. The distinguishing feature in rainfall (Figure 8, top) is the negative equatorial anomaly that persists both in sign and duration from Dec0 to Jan1 to its decline in Jun1to Jul1. There are significant off-equatorial precipitation anomalies as well at various times, most notably the one located over southern Brazil between $20°$ and $30°S$ throughout the Oct0 to May1 period, and also the positive anomaly in the subtropical north/northwest Atlantic (around $30°N$) from Feb1 through May1. Another significant feature is the dramatic increase in near-equatorial precipitation anomalies of both signs from Feb1 to Mar1 and Apr1 to May1. This is due to the ITCZ transitioning from a magnitude anomaly in Feb1 to Mar1 to a magnitude and meridional displacement anomaly in Apr1 to May1; recall the results of section 2.4, which showed the abrupt northward displacement of the Atlantic ITCZ maximum position on Apr1 for the Walker composite. The positive anomaly of the precipitation dipole has an extension near the Caribbean region centered on $25°N$; *Saravanan and Chang* [2000] pointed to this Caribbean extension as a significant aspect of their AGCM simulation of tropical Atlantic variability. The bulk of the positive anomaly, but not the Caribbean extension, persists from Jun1 to Jul1. We discuss the mechanics of the positive anomaly in some detail in section 3.2.

[34] The corresponding evolution for SST and near-surface (10 m) winds is shown in Figure 8 (middle). The significant feature in the early period (Oct0 to Nov0 and Dec0 to Jan1) is the lack of anomalies in the tropics, in contrast to development in the precipitation field. This strongly suggests a nonlocal cause for the observed equatorial precipitation anomalies: the anomalous Walker circulation. Onset of northern subtropical near-surface wind anomalies occurs in Jan1 with the weakening the wind strength in the northern tropical basin. This is associated with the development of a warm SST anomaly off the west coast of North Africa in Feb1 that then appears to expand westward into the interior of the basin; NS96 also noted the westward expansion of northern tropical Atlantic SST anomaly. This warming of the northern tropical Atlantic SST anomaly forms an anomalous cross-equatorial SST gradient that maximizes in Mar1 (Figure 6c). The lag in the northern tropical Atlantic SST response with respect to the initial wind response is consistent with previous studies [NS96; *Enfield and Mayer*, 1997], concluding that SST change in this region is caused by surface flux anomalies due to changes in trade wind magnitude.

[35] The pattern of SST and winds changes after the onset of the first SST anomalies in Feb1. The northern subtropical wind anomalies die down by Mar1. The decline of the northern subtropical wind anomaly coincides with the peak in northern tropical SST anomaly, which in its turn decays after Apr1 to May1. Cold SST anomalies in the southern subtropics form off the coast of southwest Africa in Mar1, followed by the onset of cold equatorial SST anomalies in Apr1. Both centers of cold SST anomalies merge and decay after the Apr1 to May1 period.

[36] The cross-equatorial flow near the equator,the trademark feature of the dominant mode of tropical Atlantic interannual-decadal variability [*Sutton et al.*, 2000; *Chang et al.*, 2000], develops in sync with the tropical SST meridional gradient anomaly. These winds are characterized by southeasterly flow over the equator, changing to a northward direction around $5°$–$10°N$. They peak in Apr1, lagging the maximum SST gradient time of Mar1 by 1 month. *Curtis and Hastenrath* [1995] also found that the cross-equatorial winds associated with warm ENSO events peak in Apr1. This anomalous cross-equatorial wind pattern weakens the wind speed just north of the equator (equator to $10°N$) by 0.5–1 m/s and strengthens the wind speed just to the south of it (equator to $10°S$) by 1–2m/s (Figure 8, bottom).

2.5.2. Gradient anomaly composite. [37] Figure 9 (top) shows precipitation anomalies for the gradient anomaly com-

posite in a format similar to Figure 8. The striking feature in this case is the positive-negative dipole in precipitation anomalies that starts in Jan1 and persists through May1 (Figure 9, top). The positive northern part of the dipole extends into Jun1, while the negative southern part reduces to a small region over northeast Brazil. There are negative precipitation anomalies over the northern tropical Atlantic in Oct0 and Nov0 and over the equatorial western Atlantic in Dec0 and Jan1, but the magnitudes are small, and they are not significant. Other notable features of the precipitation are the positive anomalies over southeast Brazil extending into the southern tropical Atlantic in Jan1 and Feb1 and also an intense positive anomaly on the equatorial west coast of Africa in Jun1 and Jul 1. Note also the lack of precipitation anomalies in the northern and southern subtropics during Feb1 to Mar1 and Apr1 to May1, in contrast to the Walker anomaly composite (Figure 8, top). This difference reflects the influence of the ENSO "atmospheric bridge" effect in the subtropics.

[38] Figure 9 (middle) shows corresponding SST and wind vector anomalies, and Figure 9(bottom) shows the wind speed anomalies. The meridional gradient in SST appears in Jan1 (this is not obvious from the bimonthly resolution of Figure 9 but is apparent at monthly resolution. Also, see Figure 6d). Both the northern and southern tropical SST anomalies increase in magnitude, with the northern tropical SST anomaly persisting through Apr1 to May1 before dying down in Jun1 and Jul1, whereas the southern tropical SST anomaly starts decaying sooner, in Apr1 and May1. The SST gradient is substantially maintained from Jan1 through May1. Intense westerly-southwesterly wind anomalies occur in Jan1 over the northern tropical Atlantic, reducing wind speed over the region (Figure 9, bottom). Southeasterly wind anomalies in the southern tropical Atlantic occur 1 to 2 months later in Feb1 and Mar1, leading to strengthened wind speeds and are concurrent with cooler SST anomalies over the west coast of Africa around $10°S$ and also over the western and central subtropical Atlantic around $20°S$.

[39] The cross-equatorial flow is already apparent in Dec0 and Jan1 and persists through to Jun1 and Jul1. Like the Walker anomaly composite, the strength of the cross-equatorial flow follows closely the strength of the SST gradient anomalies. Furthermore, the effect of the cross-equatorial winds on wind speed is to reduce wind speed over the tropical Atlantic just north of the equator (from the equator to $10°N$) by 0.5–1 m/s and to increase wind speed just south of the equator (from the equator to $10°S$) by 0.5–1.5 m/s.

[40] We comment on the presence of the apparent "dipole" in the SST anomaly in reference to the ongoing debate about its existence [*Houghton and Tourre*, 1992; *Xie and Tanimoto*, 1998; *Enfield et al.*, 1999]. In our analysis it is simply there by construction since we chose the composite years on the basis of the TAG index, which will have extreme values when the one hemisphere is anomalously warm and the other is anomalously cold. Thus our analysis does not lend or remove support for the existence of the dipole.

2.6. Summary of Observational Results

[41] Our observational analysis suggests that, to first order, the Walker circulation mechanism acts to suppress near-equatorial Atlantic rainfall. Two features of our results support this qualitative interpretation:

1. The Walker composite of the ITCZ time series in section 2.4 shows that precipitation magnitude is significantly reduced in Walker years from Dec0 to Feb1, when the Walker mechanism is strong but the gradient mechanism is weak. The results suggest a reduction of between 20 and 40% in the monthly precipitation averaged over the region $15°S$ and $20°N$ and $35°W$ to $15°W$, compared to climatology.
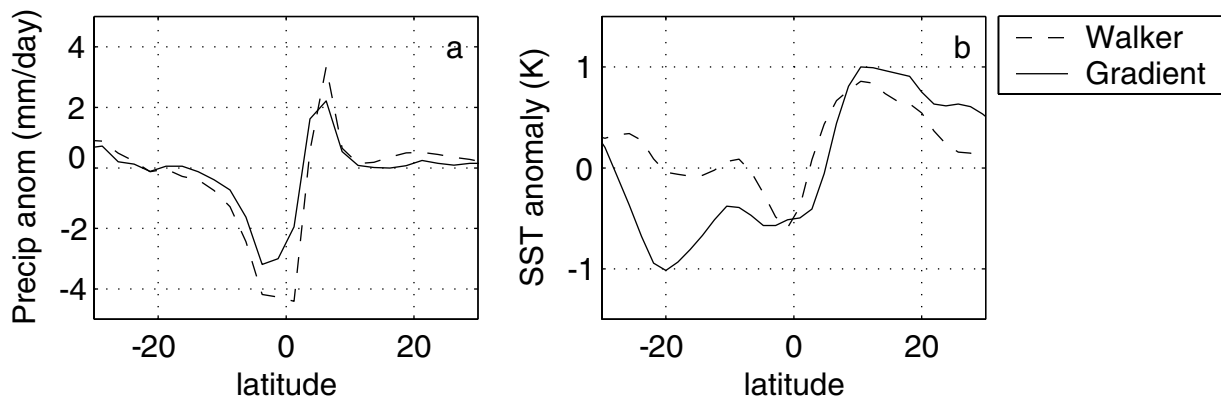
Figure 10. (a) Precipitation and (b) SST anomalies averaged between 35°W and 15°W and from Apr1 to May1 for the Walker (dashed curves) and gradient (solid curves) cases.

2. The Walker anomaly composite in section 2.5 shows that near-equatorial rainfall is suppressed over Dec0 and January and Feb1 and Mar1. This occurs despite the absence of significant SST and wind anomalies directly below the precipitation.

[42] We also note an apparent time lag, on the order of 1 month, between the peak in the convective forcing in the eastern equatorial Pacific and the peak in the anomalous precipitation response. Our observational results also show that the gradient mechanism positions the ITCZ maximum. The features of our results that support this qualitative interpretation are as follows:

1. The gradient composite described in section 2.4 shows that the difference in maximum ITCZ position is most significant between Feb1 and Jun1, overlapping the period when the gradient influence is largest.

2. The gradient anomaly composite for section 2.5 corroborates the results for section 2.4, showing the largest ITCZ displacement patterns in Feb1 to Mar1 and Apr1 to May1.

3. The onset of significant northward displacement in the Walker anomaly composite occurs in Apr1 but only after the onset of strong SST gradients in Mar1. Unlike the precipitation response to the Walker mechanism, the anomalous ITCZ displacement does not appear to significantly lag the SST gradient forcing in time.

2.7. What Happens to the ITCZ When Both the Walker and Gradient Mechanisms Are Active?

[43] In the Walker anomaly composite, both the Walker and gradient influences are strong between Mar1 and May1. Is the response a linear combination of the two influences, or are there nonlinear effects that make interpretation nontrivial?

[44] The Mar1 situation appears to be nontrivial because of the lack of a significant negative response in tropical Atlantic rainfall magnitude at that time despite the strong Walker influence. This could indicate problems with our assertion that the Walker circulation suppresses remote rainfall. However, since the gradient influence is also strongly acting, we contend that the interaction between the two mechanisms may lead to a nonlinear outcome.

[45] We discuss in greater depth the situation for Apr1 to May1 in the Walker anomaly composite (Figure 8). This has direct bearing on the analysis of a previous study [*Chiang et al.*, 2000], which addressed the ENSO influence on April-May northeast Brazil rainfall (a good proxy for the state of the Atlantic

ITCZ). In that study we hypothesized a Walker circulation influence on the April-May northeast Brazil rainfall in addition to the gradient influence to which the variation in rainfall is usually attributed. What do our current results say in retrospect?

[46] To aid us in our interpretation, we calculate the zonal average between 35°W and 15°W of the precipitation and SST anomalies shown in Figures 8 and 9 (Walker and gradient anomaly composite) for Apr1 and May1. The meridional profiles for precipitation (Figure 10a) are similar, except that the amplitude is larger in the Walker anomaly composite, especially the negative anomaly at and just south of the equator. The SST profiles (Figure 10b) show, consistent with the results of Figure 6, that the north-south hemispheric difference in SST anomalies (which is how the TAG index is defined) is only half as large in the Walker anomaly composite (although the size of the cool equatorial SST anomaly is comparable). The implication is that the gradient mechanism cannot explain all of the precipitation response in the Walker anomaly composite and that part of the response in precipitation should be attributable to the direct Walker influence. Most of this additional response appears to be suppression of rainfall in the negative half of the precipitation dipole, consistent with earlier results that showed suppression of near-equatorial rainfall when the Walker mechanism acted alone. *Saravanan and Chang* [2000] showed a similar result in their AGCM study when they tried to isolate the Walker influence on the Atlantic ITCZ. Note also the larger and slightly more northward positive peak in the precipitation dipole for the Walker anomaly composite as compared with the gradient anomaly composite. This suggests that the Walker mechanism may also act to displace the ITCZ maximum northward during April and May. If this displacement is indeed real, it still represents a secondary effect to the suppression of rainfall in the near-equatorial region.

[47] The conclusion aids the interpretation of the result by *Chiang et al.* [2000] concerning the relative influences of the Walker and gradient mechanisms on northeast Brazil rainfall. Figure 11 reproduces the scatterplot in Figure 5 of *Chiang et al.* [2000], which shows an index for April-May northeast Brazil rainfall (labeled "CPI AM" in Figure 11; see *Chiang et al.* [2000] for definition of the index) versus an index for the strength of April-May convection in the eastern equatorial Pacific (labeled "pNiño3AM" in Figure 11; see *Chiang et al.* [2000] for definition of the index). Figure 11 basically shows the control that eastern equatorial Pacific heating has on the range (in particular, the maximum) of April-May northeast Brazil rainfall. When the Walker influence is small (low pNiño3AM), northeast Brazil rainfall is controlled by the SST gradient that acts to position the ITCZ maximum. With increasing Walker influence the suppression of ITCZ precipitation over the equator and to the south (northeast
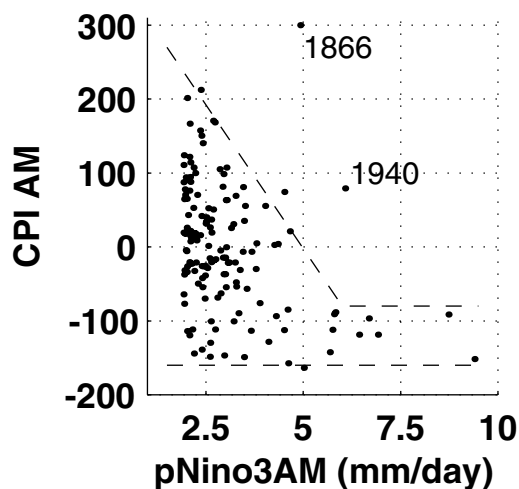
Figure 11. Scatterplot of an index of northeast Brazil April-May rainfall (the CPI AM index of *Chiang et al.* [2000]) versus a proxy of April-May eastern Pacific convective heating (the in pNiño3AM index) over 1856–1998. The dashed lines represent the approximate range of CPI AM for given pNiño3AM. The dates for two outliers are also shown. Taken from *Chiang et al.* [2000, Figure 5].

Brazil is between ~2°S and 10°S) reduces the upper limit that northeast Brazil rainfall can take.

3. Mechanisms

[48] In this part of the paper we attempt to explain on the basis of present understanding of tropical interactions how the Atlantic ITCZ is influenced. Our discussion for the Walker influence is short because previous work on the details of this mechanism is surprisingly limited despite the widespread use of the concept of the Walker circulation. We dedicate more discussion to the gradient mechanism, for which a theory has been previously proposed (HG93).

3.1. Walker Mechanism

3.1.1. Tropospheric warming. [49] The conceptual idea of the Walker circulation influence on remote convection is the suppression of remote rainfall via stabilization of the atmospheric column through tropospheric warming. The net warming of the mean tropical tropospheric temperature of around 0.5–1 K during El Niño years is well known and has been shown to be linked to convective heating in the tropical Pacific [*Yulaeva and Wallace*, 1994]. Because the tropical atmosphere cannot support large temperature gradients, the heating of the tropical Pacific atmosphere spreads rapidly through the entire tropical troposphere [*Wallace*, 1992]. *Yulaeva and Wallace* [1994] estimate a time frame of around 3 months from the onset of the anticyclone pair associated with convection in the eastern equatorial Pacific to the net warming over the entire tropical troposphere.

[50] Our own analysis of NCEP temperatures between 35°W and 15°W for the Walker anomaly composite shows significant warming in tropical Atlantic above 750 mbar, consistent with the heating influence of anomalous eastern Pacific convection (Figure 12). The warming occurs over a narrow 5°S to 5°N band in Jan1 but widens to beyond 10°S–10°N by Mar1. The equatorially confined nature of the initial warming signal and the subsequent widening are consistent with a transient Kelvin wave response to the eastern equatorial Pacific heating. Furthermore, the time lag in the adjustment (1–2 months) is roughly consistent with the 3-month lag as found by *Yulaeva and Wallace* [1994]. The amplitude of the anomalous tropospheric temperatures we find is up to 1°C in the peak warming period of Apr1, the magnitude of which is comparable with those found by Yulaeva and Wallace. The warming leads to a stabilization of the atmospheric column and is consistent with the effect on ITCZ precipitation.

3.1.2. Why boreal spring is important. [51] Note that the difference in eastern Pacific near-equatorial heating between Walker and background years maximizes in late boreal winter and early spring (Figure 6a). This is the warmest period in the climatological seasonal cycle of SST in the eastern equatorial Pacific, so total SST associated with warm ENSOs usually peaks around this time. Given that there is a slight (1–2 month) lag in the anomalous tropospheric temperature response, this implies that boreal spring is the time when the Walker mechanism will have maximum influence on tropical Atlantic precipitation

[52] Boreal spring is also the time when the Atlantic ITCZ is most sensitive to the Walker mechanism. The Atlantic ITCZ is closest to the equator during boreal spring, and furthermore, it is also at its most variable state in terms of magnitude (see Figure 2). Thus even though the initial tropospheric warming caused by Pacific heating may be confined to the near-equatorial region, the Atlantic convection is sufficiently close to the equator to be influenced by it. The proximity of the Atlantic ITCZ to the equator at the time of peak Walker influence is no coincidence, as the seasonal evolution of both the eastern Pacific and Atlantic ITCZs is related to solar forcing and ocean-atmosphere interac-
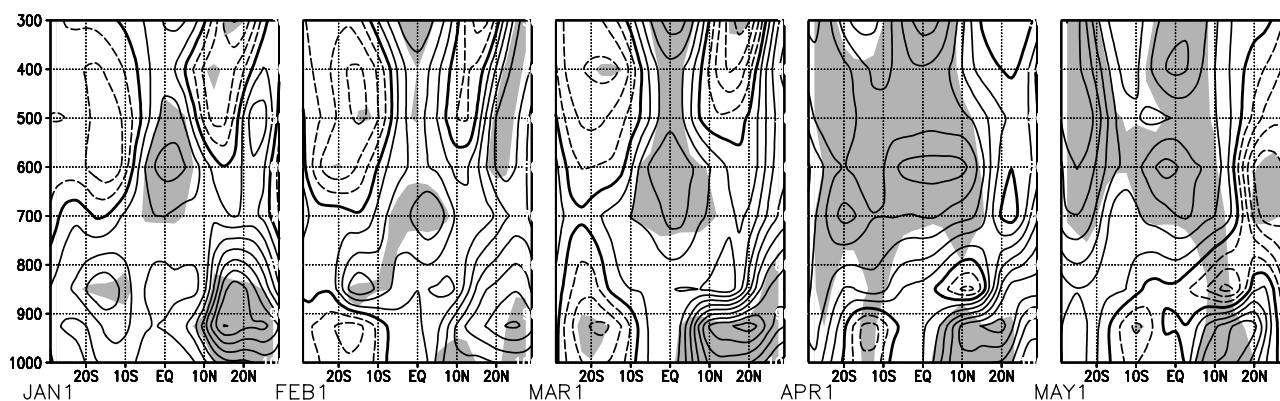

Figure 12. Walker anomaly composite tropospheric temperatures zonally averaged between 35°W and 15°W and from Jan1 to May1. Shading indicates significance at the 10% level. The contour interval is 0.2 K, and negative anomalies are dashed.
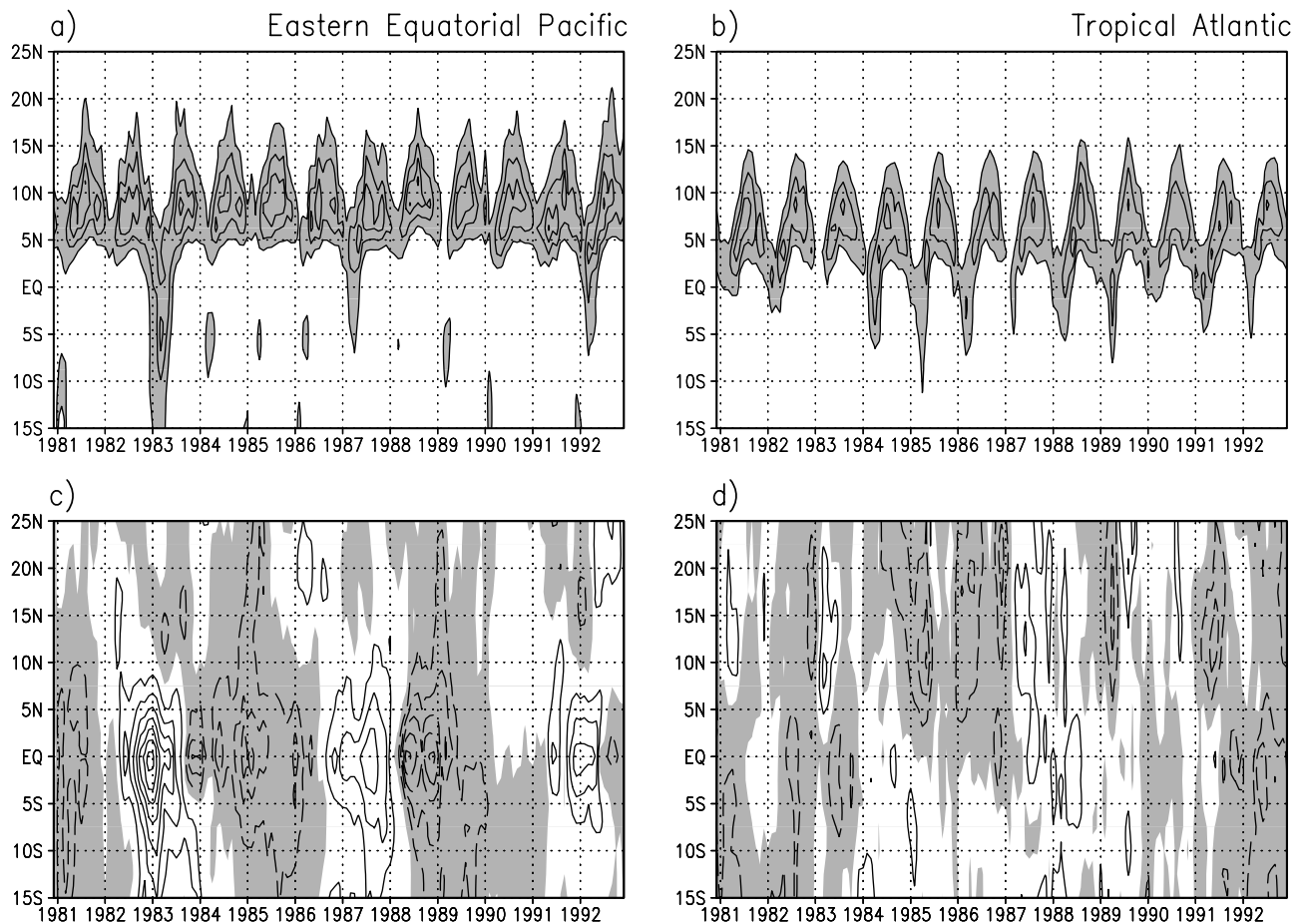
Figure 13. (top) Latitude-time plots for the (a) eastern Pacific and (b) Atlantic ITCZs. Eastern Pacific precipitation is zonally averaged between 160°W and 90°W, and tropical Atlantic precipitation is zonally averaged between 40°W and 0°W. Contour interval is 4 mm/d, and values above 4mm/d are shaded. (bottom) Latitude-time plots for the zonally averaged SST anomaly in the (c) eastern Pacific and (d) Atlantic. The zonal averaging is done over the same regions as for the respective ITCZs. Contour interval is 0.5 K, and negative values are shaded.

tions governing the ITCZ and cold tongue dynamics [*Wang and Wang*, 1999].

3.2. SST Gradient Mechanism

[53] HG93 proposed an explanation for gradient influence on the ITCZ location which can be summarized as follows: they refer to the theory of *Lindzen and Nigam* [1987], whereby a cross-equatorial SST gradient causes a meridional pressure gradient across the equator in the Atlantic through differential heating of the boundary layer. This surface pressure drives cross-equatorial meridional winds that are assumed to affect the position of the ITCZ. Thus HG93 state a direction of causality; SST gradient causes cross-equatorial winds, which then position the convection.

[54] While we believe HG93 are correct, to first order, there are many features to the variability of the ITCZ that are not explicitly addressed. First, a theory for Atlantic ITCZ variability needs to explain the seasonality of the behavior. Our results and others (e.g., NS96) show that the largest ITCZ displacements occur in March and April, despite the fact that the SST gradient in the gradient anomaly composite (see Figure 6d) is strong from January through June.

[55] Second, the Atlantic ITCZ displacement is quite sensitive to relatively small variations in the SST gradient. Contrasting it with its counterpart in the eastern Pacific best highlights this point. Figures 13a and 13b show Hovmoeller diagrams of the two ITCZs between 1979 and 1999, zonally averaged over the appropriate regions (160°W to 90°W for the eastern Pacific and 40°W to 0°W

for the Atlantic) of the tropical oceans. Like the Atlantic ITCZ, the largest variability in the eastern Pacific ITCZ is also manifested as a meridional displacement of its southernmost extension in boreal spring. Variability in the Pacific ITCZ is "bimodal" in the sense that the maximum southward displacement in any given year either stays well clear of the equator or penetrates fully to the equator and into the Southern Hemisphere (Figure 13a). By contrast, the maximum southward extent of the Atlantic ITCZ occupies more of a continuum of latitudes north and south of the equator (Figure 13b). The southerly excursions of the Pacific ITCZ are clearly associated with El Niño events, which are associated with equatorial SST changes on the order of 2° to 4° (Figure 13c). By comparison, SST changes associated with comparable Atlantic ITCZ displacements are much smaller, on the order of 0.5° and furthermore, they occur poleward (north and south) of the equator (Figure 13d).

[56] Third, HG93 treat the ITCZ simply as tracer for the boundary layer controlled surface circulation. This is in stark contrast to the role of convection in ENSO, where it is thought to play an intimate role in the positive feedback by driving anomalous equatorial trades that ultimately affect eastern Pacific SST through ocean dynamics and thermodynamics. In the extreme case it is conceivable that an initial Atlantic ITCZ displacement may act to trigger the SST gradient anomaly, reversing the cause and effect linkage implicit in the HG93 mechanism. Even if HG93 are correct in that the SST gradient initiates the displacement in the

ITCZ, the ITCZ may influence the behavior through impacting the tropical Atlantic SST which, in turn, may feed back onto the ITCZ. Do our results say anything about the scope and strength of this feedback?

[57] A more complete theory for how the SST gradient influences the Atlantic ITCZ must answer these key questions:

1. Why does ITCZ variability peak in boreal spring?

2. Why is the character of ITCZ variability in the tropical Atlantic different from that of the eastern Pacific? In particular, why is the Atlantic ITCZ so sensitive to small anomalous SST gradients?

3. What is the role of the ITCZ in the life cycle of the tropical Atlantic gradient? In particular, is the ITCZ displacement a cause or consequence of the SST gradient? If it is a consequence of the SST gradient, then does the ITCZ displacement impact the local SST anomaly and feed back on the gradient?

3.2.1. The importance of the basic state ocean conditions. [58] We think the answer to the seasonality of Atlantic ITCZ variability lies with the mean state of the ocean surface during boreal spring. The period of largest ITCZ variability (February–April) coincides with the time of year when the meridional SST profile over the equatorial region is "flat" (Figure 14, Feb-Mar and Apr-May, solid curves). Since the latitudinal extent of the ITCZ is about half of this flat region in SST, the suggestion is that the ITCZ position can be variable at this time because the underlying SST can support convection over a wider range of latitudes. On the other hand, the cold tongue in the Pacific is present in the mean even in boreal spring, and only a sizable ($\sim 1-2$ K) equatorial SST anomaly is able to "flatten" the boreal spring eastern Pacific SST (Figure 14, dashed curves). This explains why the Pacific ITCZ reaches the equator only during sizable El Niño events. The importance of the basic state is highlighted through a coupled model study (M. Biasutti, personal communication, 2000). They show that the fully coupled climate system model does not display the observed ITCZ seasonal behavior and variability; a fact they attribute to the poor basic state tropical Atlantic Ocean surface temperature simulation. When they move to an AGCM coupled to a slab ocean (where the mean ocean surface temperature is specified through a flux correction), they reproduce very well the seasonal behavior and variability of the Atlantic ITCZ.

[59] Hence the question of why the ITCZ position is most variable in boreal spring is a question of why the basic state seasonal cycle of the ITCZ and cold tongue behaves the way it does. The key features of Atlantic ITCZ variability rely on its relative location to, and strength of, the cold tongue. The region of most variability is located in the western half of the basin, where the cold tongue influence is the weakest. The difference between the Atlantic and Pacific cold tongue strength is attributable to the zonal size of the basin [*Zebiak*, 1993], the larger size allowing for a greater fetch as the equatorial easterlies act to pile the surface waters to the western end of the tropical basin and shoal the thermocline to the east.

3.2.2. How can a small SST anomaly make such a big difference? [60] The basic state meridional SST profile explains the potential for the ITCZ to shift, assuming an SST threshold above which convection can occur. However, it does not explain why it should vary; indeed, how do small SST anomalies, as characterized by the equatorial SST gradient, make such a big difference to the position of convection? It is unlikely that the precipitation difference can be explained purely from thermodynamical considerations alone. However, the anomalous cross-equatorial SST gradient can and does produce surface pressure gradients, albeit weak, as HG93 showed. What makes the cross-equatorial surface pressure gradient so effective at driving cross-equatorial winds is the frictionally dominated surface
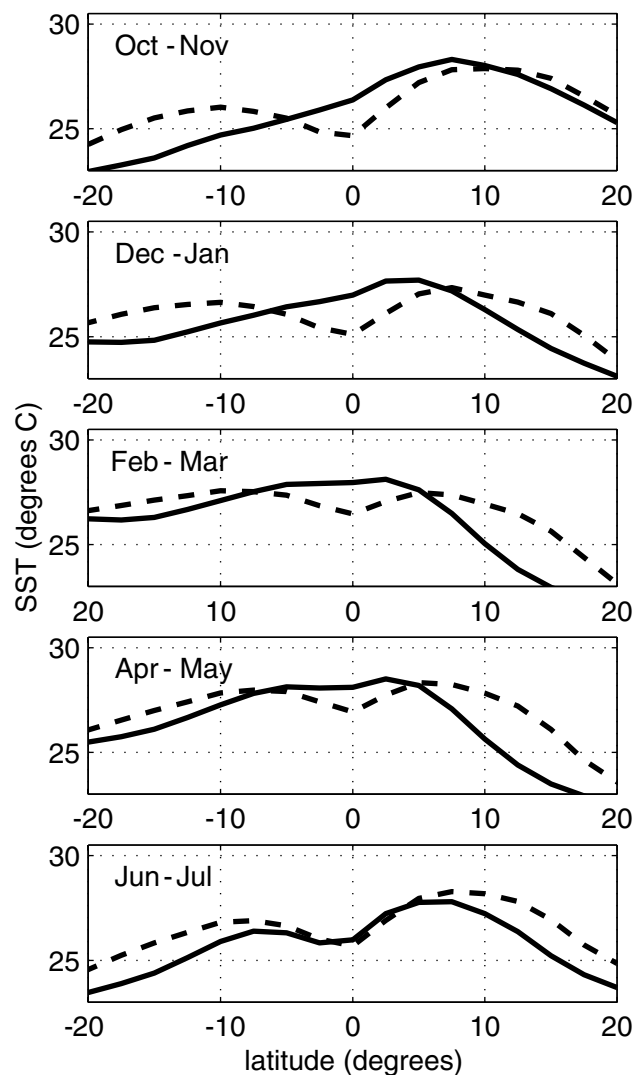

Figure 14. Meridional profile of zonally averaged SST over the Atlantic basin between 40°W and 0°W (solid line) and for the Pacific basin zonally averaged between 160°W and 90°W. The profiles shown are two-month climatological means in time sequential order top to bottom, starting from October-November.

momentum balance near the equator [*Deser*, 1993]. Sizable (on the order of $1-2$ m/s) boundary layer meridional winds will occur near the equator to try to damp this pressure gradient down. In contrast, the SST anomalies generated in the eastern equatorial Pacific are symmetric about the equator and do not affect the meridional pressure gradient there.

[61] The boundary layer meridional wind by itself does not influence the position of convection; rather, it is the ability of the surface winds to modify the moist static energy in the boundary layer. To illustrate this, we show the gradient anomaly composite meridional: the height profile of anomalous moist static energy from just prior to the onset of significant SST gradients in Dec0 through Apr1 when the gradient is fully established (Figure 15). Substantial positive anomalies occur in the boundary layer near 10°N in Jan1 with the onset of a significant meridional SST gradient (see Figure 6d) and before a significant anomaly in the position of convection develops (Figure 7d). In contrast, the atmosphere above the increased moist static energy shows no significant response. The implication is that the atmosphere has become less stable to convection north of the equator. This condition persists through Apr1 and beyond, although in the
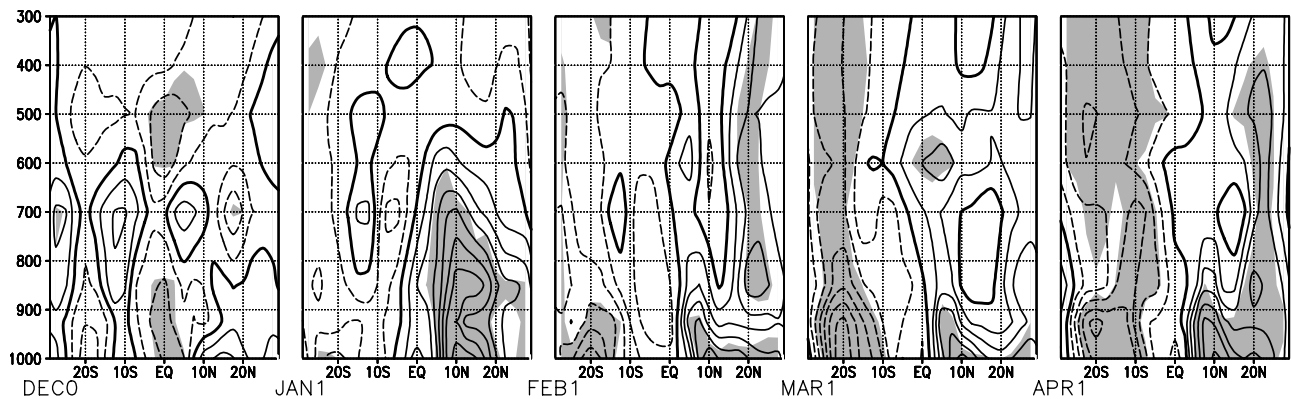
Figure 15. Gradient anomaly composite moist static energy zonally averaged between 35°W and 15°W and for Dec0, Jan1, Feb1, Mar1, and Apr1. Contour interval is 500 J/kg, negative contours are dashed, and significance at 10% level is shaded.

months subsequent to Jan1 the boundary layer increase in moist static energy is confined to a much shallower layer (<900 mbar) near the surface. This may be a consequence of the onset of anomalous convection there. Note also the onset of significant negative moist static energy anomaly near the surface between 10°S and 30°S in Feb1, which coincides with the onset of colder than usual south tropical Atlantic SST. In Mar1, with the onset of significant northward ITCZ displacement, the negative anomaly in the southern tropics extends throughout the depth of the troposphere (at least up to 300 mbar). This extension is likely due to the drying out of the atmosphere from anomalous subsidence associated with the meridional ITCZ displacement.

[62] The increase of moist static energy in the boundary layer is primarily due to the increase in specific humidity, and the latitude-height structure of specific humidity closely resembles the boundary layer convergence (not shown). We interpret this to mean that the change in boundary layer specific humidity is determined primarily through moisture flux convergence brought about through the wind convergence. What is special about surface winds in near-equatorial regions is how the linear surface momentum balance, which generally applies to anomalous flow over the tropical oceans, transitions from subgeostrophic flow near the equator to a largely geostrophic balance away from it. Northward cross-equatorial meridional winds driven by meridional pressure gradients veer to the right, north of the equator under the Coriolis effect, resulting in surface wind convergence. Conversely, the flow toward the equator in the south produces divergence. This admittedly oversimplified physical picture is a linearized version of the "convergence-divergence doublet" explanation proposed by *Tomas and Webster* [1997, p. 1445] (see also *Tomas et al.* [1999]) to explain the role of cross-equatorial pressure gradients in influencing the location of near-equatorial convection). In their more complete picture the boundary separating the convergence region from the divergence is determined by the zero absolute vorticity contour rather than the equator; this allows for the possibility for this doublet to be centered away from the equator because of advection of absolute vorticity by the mean flow.

[63] *Hastenrath and Lamb* [1977] showed the association between cross-equatorial flow and the location of convergence/divergence for the mean flow in the tropical Atlantic during July-August: they pointed out that the latitude of recurvature in the southeasterly trades (i.e., the latitude of no zonal wind) at ~5°N separated a region of convergence to the north of it from a region of divergence to the south. It is likely that when HG93 discussed the anomalous cross-equatorial flow and assumed its linkage to location of ITCZ convection that they had this picture in mind, although this was not explicitly stated.

3.2.3. ITCZ displacement and cross-equatorial flow. [64] If we assume that cross-equatorial meridional winds

determine the location of ITCZ convection, then the question of how much the ITCZ directly influences its own position is largely a question of how much influence the ITCZ has on cross-equatorial winds. *Chiang et al.* [2001] investigated this question by driving a linear primitive equation model with convective and surface forcing characteristic of the peak phase of tropical Atlantic gradient variability. They found that for time-mean anomalous near-equatorial flows the SST gradient is the dominant driver of the cross-equatorial meridional wind response, whereas elevated heating is the dominant driver of the zonal flow. This result suggests that it is the cross-equatorial SST gradient that initiates the ITCZ displacement and not the other way around. This interpretation is supported by the observational results in both our Walker and gradient anomaly composites: in both cases the cross-equatorial winds develop in tandem with the anomalous cross-equatorial SST gradient, and the ITCZ displacement occurs only during or after the onset of strong anomalous SST gradients. If cause and effect were reversed, then the SST anomaly response should lag the ITCZ displacement (and associated anomalous cross-equatorial winds) because of the thermal inertia of the ocean.

[65] However, as *Chiang et al.* [2001] show, the displaced ITCZ does contribute to some of the cross-equatorial wind response, suggesting that there is a second-order effect of the ITCZ acting to maintain its anomalous displacement. There is also another route for positive feedback, which we describe below.

3.2.4. Feedback on the SST gradient. [66] *Chang et al.* [1997] proposed a tropical Atlantic ocean-atmosphere mechanism for self-sustaining decadal timescale oscillations for the TAG through positive feedback between the cross-equatorial winds and the meridional gradient in SST. However, more recent simple model studies, notably by *Xie and Tanimoto* [1998] and a more detailed model study by *Chang et al.*[2001], have suggested that the TAG results from a damped mode forced by extratropical noise. In particular, *Chang et al.* [2000, 2001] suggest that significant positive feedback between cross-equatorial winds and the SST gradient occurs only in the "deep tropics" (between ~10°N and 10°S). Yet others [e.g., *Sutton et al.*, 2000] do not find evidence for positive feedback.

[67] We come to a conclusion similar to that of *Chang et al.* [2000, 2001] with regards to the region of significant two-way air-sea coupling on the basis of our observational results. It is clear from both the Walker and gradient anomaly composites (see Figures 8 and 9) that the Northern Hemisphere subtropical trade wind anomalies occur before the peak in the northern tropical SST anomalies, suggesting (in agreement with NS96) an atmospheric origin for them. The trade wind counterpart for the Southern Hemisphere in the gradient anomaly composite appears to occur simultaneously (at monthly resolution) with the cooler SST anomaly in Feb1-Mar1; however, the trade wind anomalies disappear in

Apr1-May1 while the cool SST anomalies are still present, implying that the winds here are also not a response to the SST anomalies. On the other hand, the deep tropical cross-equatorial wind response (between ~10°S and 10°N) in both the Walker and gradient anomaly composites occurs in sync with the anomalous SST gradient; indeed by late boreal spring (Apr1-May1) there are no subtropical trade anomalies, but the deep tropical response is clearly present. Thus our results suggest that the deep tropical cross-equatorial wind response is the only definite atmospheric response to the anomalous SST gradient and associated anomalous convective forcing. This interpretation is supported by the idealized model study of *Chiang et al.* [2001], which showed that only the near-equatorial wind response could be reasonably well simulated in a tropical atmosphere model forced by anomalous SST and convective forcing representative of peak anomalies of the tropical Atlantic gradient mode.

[68] We used NCAR-NCEP reanalysis fluxes to obtain estimates of the surface flux feedback for the gradient anomaly composite. The net surface flux (shortwave plus longwave plus latent plus sensible) during the months of peak cross-equatorial winds (Mar1-Apr1) is between 10 and 30 W/m^2 into the ocean for the northern tropical Atlantic between the equator and 10°N and between 0 and 20 W/m^2 out of the ocean for the southern tropical Atlantic between the equator and 15°S. The majority of this flux response for both cases comes from anomalous latent heat fluxes, with a small but complementary contribution from anomalous sensible heat fluxes. Assuming a typical mixed layer depth of 50 m, the SST change due to the surface flux anomaly of 20 W/m^2 is ~0.25 K/month. However, the SST change in the vicinity of the maximum surface flux anomaly is generally much less that that, implying that ocean heat transports are acting to damp the anomalies. This interpretation of the role of ocean heat transport is consistent with the results of studies by *Seager et al.* [2000] and *Chang et al.* [2001]. Hence we suggest that the role of the positive surface flux feedback in TAG is to prolong an existing anomalous cross-equatorial SST gradient into the boreal spring and summer. However, the strong damping by the near-equatorial ocean heat transport damps effectively the positive surface flux feedback.

4. Summary and Discussion

[69] We analyzed interannual Atlantic ITCZ variability beginning with the hypothesis of two dominant influences, namely, that of the local meridional SST gradient and that of the anomalous Walker circulation related to the remote El Niño–Southern Oscillation (ENSO) phenomenon. We analyzed the position of maximum ITCZ precipitation and precipitation magnitude and associated SST and surface wind behavior between 1979 and 1999 using composites representative of each influence. The difficulty with isolating each mechanism comes from the fact that both appear to be active during ENSO events. We managed a partial isolation by applying two tactics: first, a judicious choice of indices representing each influence and second, exploitation of the time-dependent evolution of each influence. We assessed the strength of the Walker circulation through measuring the magnitude of precipitation anomalies in the eastern Pacific, symmetric about the equator, in accordance with the requirements of equatorial dynamics. For the SST gradient influence we chose an interannual index considering the year-round evolution of the gradient from its onset in boreal spring and through the following summer. Our main result is that to first order, the Walker circulation suppresses rainfall in the tropical Atlantic, whereas the cross-equatorial SST gradient influences the meridional position of maximum precipitation.

[70] We analyzed a composite situation for April and May when both the Walker and the warm north/cool south gradient mechanism are acting strongly on the Atlantic ITCZ. Our results suggest that the dipole ITCZ precipitation anomaly cannot be attributed solely to the gradient mechanism, and that part of the dipole response, especially the precipitation deficit to the south, is a consequence of the Walker mechanism. This supports the assertion of the recent paper by *Chiang et al.* [2000] that the Walker mechanism is modulating northeast Brazil rainfall. We noted that the combined response to both mechanisms might not be a linear combination of the response to each individual forcing; this appeared to be the situation for the March response in precipitation.

[71] We analyzed the dynamics underlying these mechanisms using the results of our composites. With the Walker mechanism, increased precipitation in the eastern equatorial Pacific is found to be associated with warming in the middle and upper troposphere, with a time lag of 1−2 months. This result is consistent with previous studies showing the link between variability of eastern Pacific convection and tropospheric temperatures [e.g., *Yulaeva and Wallace*, 1994] and suggests that suppression of tropical Atlantic rainfall is a consequence of the increased vertical stability of the atmospheric column due to eastern Pacific heating.

[72] Results of the gradient anomaly composite support the mechanism proposed by HG93 for how the SST gradient influences ITCZ position through driving cross-equatorial winds. This mechanism, however, does not explain (1) why ITCZ variability exhibited a seasonal dependence, (2) why the ITCZ is sensitive to relatively small anomalous SST, (3) how cross-equatorial winds position the ITCZ, and (4) what role the ITCZ plays in this mechanism. We argued that (1) the seasonal dependence of the ITCZ variability is a result of the meridionally "flat" climatological SST gradient in boreal spring that allows the ITCZ to occupy a relatively wide range of latitudinal positions; (2) that the ITCZ is sensitive to small anomalous SST gradients because near the equator, small pressure gradients are sufficient to drive significant cross-equatorial flow; (3) that the cross-equatorial flow positions the ITCZ because it produces a "convergence-divergence doublet" [*Tomas and Webster*, 1997; *Tomas et al.*, 1999] and increasing boundary layer moist static energy in the region of anomalous convergence; (4) that convection does not initiate ITCZ displacement, as it is not effective in driving cross-equatorial winds, but that it may help maintain the displacement once it is in effect; and (5) that positive feedback on the SST gradient occurs only in the near-equatorial region (~10°S−10°N) as a result of the cross-equatorial wind response and associated surface fluxes. Despite the surface flux feedback, the SST anomalies decay by the boreal summer, which suggests that ocean dynamics are acting to damp the anomalies.

[73] We close with a few comments on the implications of our results and directions for future studies. A recent AGCM study by *Giannini et al.* [2001] investigating rainfall variability over the tropical Americas comes to a similar conclusion regarding the relative roles that the direct atmospheric bridge and local SST anomalies play in mediating the ENSO impact on Atlantic ITCZ rainfall. In particular, they also find that when warm, SST anomalies in the central and eastern equatorial Pacific persist through boreal spring (implying an active Walker mechanism); they combine with an anomalously northerly location of the Atlantic ITCZ (caused by the gradient mechanism) to give significantly drier than average conditions over northeast Brazil. It is encouraging to see that the observations and models in accord in this regard, and it bodes well for potential predictability of northeast Brazil rainfall.

[74] The concept of tropospheric warming leading to suppression of remote convection is still not widely held. If one accepts the notion that tropospheric warming can cause suppression of convection, then a crucial question to ask is whether or not a 1°C warming in tropospheric temperatures (typical for a strong warm ENSO event) is significant. This study suggests that this is indeed the case. We have preliminary results from a single column convection model that supports the observational result, and they will be presented in an upcoming study.

[75] An outstanding question is one of the relative strength and roles of the anomalous Walker circulation and PNA-mediated influences of ENSO on tropical Atlantic climate variability. We have showed in this paper that the Walker mechanism has a direct impact on the magnitude of tropical Atlantic ITCZ rainfall, but beyond that this study does not make any conclusions. The tropical Atlantic SSTA response to ENSO, that the north tropical Atlantic warms significantly in response to El Niño whereas the south tropical Atlantic response is much weaker or not significant, may argue in favor of the PNA mechanism since it can readily account for the hemispheric asymmetry. However, while the Walker mechanism is in principle symmetric about the equator, the mean climate of the tropical Atlantic is not: in particular, the ITCZ generally favors the north, whereas the cold tongue and occurrence of stratus clouds favor the south. So there is no a priori reason to assume that the response of the tropical Atlantic to the Walker mechanism is symmetric about the equator.

[76] We have left completely untouched the topic of how Atlantic ITCZ variability can affect remote conditions. Changes in tropical Atlantic convection may have an impact on the extra-tropical flow in the same way that ENSO has an impact on the PNA. Recently, *Robertson et al.*, [2000] and *Okumura et al.* [2001] made a case for this linkage to the NAO on the basis of results of AGCM experiments, and *Rajagopalan et al.* [1998] and *Ruiz-Barradas et al.* [2000] also hint at this possibility from their observational analysis of the TAG. We also wonder about the impact that Atlantic ITCZ variability has on subtropical trades that are so crucial to changing the subtropical SST. If change in the Atlantic ITCZ forces change in the magnitude of the subtropical trades, a positive feedback on subtropical SST may result. This feedback would be distinct from the deep tropical feedback identified in section 3.2.4. Our gradient composite results (Figure 9) show that while there are significant subtropical trade anomalies between Dec0 and Mar1, there are none in Apr1-May1 when the Atlantic ITCZ anomalous displacement is at maximum. This suggests that if the ITCZ does force change in subtropical winds, it occurs only between boreal winter and early spring.

[77] We have mentioned the local feedback of the ITCZ displacement on the SST gradient (section 3.2.4). Another potential impact of the ITCZ displacement is on the equatorial Atlantic SST. Note that the cross-equatorial flow in the tropical Atlantic gradient pattern has a zonal component at the equator, which *Chiang et al.* [2001] show to be driven primarily by the ITCZ displacement. A northward displaced ITCZ produces equatorial easterlies that could act to cool the equatorial SST through anomalous upwelling and thermocline displacement. The cooler equatorial SST will, in turn, reinforce the northward ITCZ displacement. This mechanism may be able to explain the linkage between meridional SST gradient variability and variability in the tilt of the equatorial thermocline as observed by *Servain et al.* [1999].

[78] It is interesting to speculate on possible implications of the convectively forced large-scale surface circulation to the nature of tropical ocean-atmosphere interaction. For ENSO, convection drives zonal surface winds that are essential to the equatorial ocean response; furthermore, the convergence in the zonal winds allows for feedback of the large-scale circulation on convection. On the other hand, for the TAG pattern the ITCZ displacement does not effectively drive cross-equatorial flow, and so the large-scale surface circulation directly forced by the ITCZ displacement does not effectively feed back on convection. In other words, for the ENSO case, latent heating is strongly involved in the feedback loop, whereas in the Atlantic ITCZ case, latent heating is weakly involved. This contrast in the way latent heating is utilized may partly explain why ENSO is such a strongly coupled ocean-atmosphere mode, whereas the TAG mode seems comparatively weak. This speculation can be contrasted to the one proposed by *Xie et al.* [1999] where the properties of the modes of the coupled system explain the relative strengths.

[79] Finally, note that our observational results do not generally support the "wind-evaporation-SST" feedback mechanism that some models [e.g., *Xie and Tanimoto*, 1998; *Xie et al.*, 1999] rely upon to explain the apparent decadal variability of the "dipole" mode in the Atlantic. The positive surface flux feedback in these simple models occurs in the core of the trades, much farther north and south from the equatorial region than our results recommend. We think this problem stems largely from the simplified "Gill-like" atmospheric dynamics used in these coupled models [cf. *Chiang et al.*, 2001]. Furthermore, we showed that (see Figures 8 and 9) SST anomalies that peak in boreal spring essentially damp out by boreal summer, suggesting that positive surface flux feedback cannot sustain the memory of a boreal spring event into the following spring. This raises an interesting question: If there is significant decadal variability generated by the tropical Atlantic "dipole" mode, then where does the memory reside between successive boreal spring events? The obvious candidate is the subsurface ocean, suggesting a need for proponents of tropical Atlantic decadal variability to focus future research there.

References

Bjerknes, J., Atmospheric teleconnections from the equatorial Pacific, *Mon. Weather Rev.*, *97*, 163–172, 1969.

Chang, P., L. Ji, and H. Li, A decadal climate variation in the tropical Atlantic Ocean from thermodynamic air-sea interactions, *Nature*, *385*, 516–518, 1997.

Chang, P., R. Saravanan, L. Ji, and G. C. Hegerl, The effect of local sea surface temperatures on atmospheric circulation over the tropical Atlantic sector, *J. Clim.*, *13*, 2195–2216, 2000.

Chang, P., L. Ji, and R. Saravanan, A hybrid coupled model study of tropical Atlantic variability, *J. Clim.*, *14*, 361–390, 2001.

Chiang, J. C. H., Y. Kushnir, and S. E. Zebiak, Interdecadal changes in eastern Pacific ITCZ variability and its influence on the Atlantic ITCZ, *Geophys. Res. Lett.*, *27*, 3687–3690, 2000.

Chiang, J. C. H., S. E. Zebiak, and M. A. Cane, Relative roles of elevated heating and sea surface temperature gradients in driving anomalous sur-face winds over tropical oceans, *J. Atmos. Sci.*, *58*, 1371–1394, 2001.

Curtis, S., and S. Hastenrath, Forcing of anomalous sea surface temperature evolution in the tropical Atlantic during Pacific warm events, *J. Geophys. Res.*, *100*, 15,835–15,847, 1995.

Dai, A. G., and T. M. L. Wigley, Global patterns of ENSO-induced pre-cipitation, *Geophys. Res. Lett.*, *27*, 1283–1286, 2000.

Deser, C., Diagnosis of the surface momentum balance over the tropical Pacific Ocean, *J. Clim.*, *6*, 64–74, 1993.

Enfield, D. B., and D. A. Mayer, Tropical Atlantic sea surface temperature variability and its relation to El Niño–Southern Oscillation, *J. Geophys. Res.*, *102*, 929–945, 1997.

Enfield, D. B., A. M. Mestas-Nunez, D. A. Mayer, and L. Cid-Serrano, How ubiquitous is the dipole relationship in tropical Atlantic sea surface temperatures?, *J. Geophys. Res.*, *104*, 7841–7848, 1999.

Giannini, A., Y. Kushnir, and M. A. Cane, Interannual variability of Car-ibbean rainfall, ENSO and the Atlantic Ocean, *J. Clim.*, *13*, 297–311, 2000.

Giannini, A., J. C. H. Chiang, M. A. Cane, Y. Kushnir, and R. Seager, The ENSO teleconnection to the tropical Atlantic Ocean: Contributions of the remote and local SSTs to rainfall variability in the tropical Americas, *J. Clim.*, in press, 2001.

Gill, A. E., Some simple solutions for heat-induced tropical circulation, *Q. J. R. Meteorol. Soc.*, *106*, 447–462, 1980.

Goddard, L., and N. E. Graham, Importance of the Indian Ocean for simu-lating rainfall anomalies over eastern and southern Africa, *J. Geophys. Res.*, *104*, 19,099–19,116, 1999.

Hastenrath, S., Upper air mechanisms of the Southern Oscillation in the tropical Atlantic sector, *J. Geophys. Res.*, *105*, 14,997–15,009, 2000.

Hastenrath, S., and L. Greischar, Circulation mechanisms related to northeast Brazil rainfall anomalies, *J. Geophys. Res.*, *98*, 5093–5102, 1993.

Hastenrath, S., and L. Heller, Dynamics of climatic hazards in northeast Brazil, *Q. J. R. Meteorol. Soc.*, *103*, 77–92, 1977.

Hastenrath, S., and P. Lamb, Some aspects of circulation and climate over the eastern equatorial Atlantic, *Mon. Weather Rev.*, *105*, 1019–1023, 1977.

Horel, J. D., A rotated principal component analysis of the interannual variability of the Northern Hemisphere 500 mb height field, *Mon. Weather Rev.*, *109*, 2080–2092, 1981.

Horel, J. D., and J. M. Wallace, Planetary-scale atmospheric phenomena associated with the southern oscillation, *Mon. Weather Rev.*, *109*, 813–829, 1981.

Houghton, R. W., and Y. M. Tourre, Characteristic low-frequency sea surface temperature fluctuations in the tropical Atlantic, *J. Clim.*, *5*, 765–771, 1992.

Kalnay, E., The NCEP/NCAR 40-year reanalysis project, *Bull. Am. Meteorol. Soc.*, *77*, 437–471, 1996.

Kaplan, A., M. A. Cane, Y. Kushnir, A. C. Clement, M. B. Blumenthal, and B. Rajagopalan, Analyses of global sea surface temperature 1856–1991, *J. Geophys. Res.*, *103*, 18,567–18,589, 1998.

Klein, S. A., B. J. Soden, and N.-C. Lau, Remote sea surface temperature variations during ENSO: Evidence for a tropical atmospheric bridge, *J. Clim.*, *12*, 917–932, 1999.

Kumar, K. K., B. Rajagopalan, and M. A. Cane, On the weakening relationship between the Indian monsoon and ENSO, *Science*, *284*, 2156–2159, 1999.

Lau, N. C., and M. J. Nath, The role of the atmospheric bridge in linking tropical Pacific ENSO events to extratropical SST anomalies, *J. Clim.*, *9*, 2036–2057, 1996.

Lindzen, R. S., and S. Nigam, On the role of sea surface temperature gradients in forcing low level winds and convergence in the tropics, *J. Atmos. Sci.*, *44*, 2418–2436, 1987.

Nobre, P., and J. Shukla, Variations of sea surface temperature, wind stress and rainfall over the tropical Atlantic and South America, *J. Clim.*, *9*, 2464–2479, 1996.

Okumura, Y., S.-P. Xie, A. Numaguti, and Y. Tanimoto, Tropical Atlantic air-sea interaction and its influence on the NAO, *Geophys. Res. Lett.*, *28*, 1507–1510, 2001.

Preisendorfer, R. W., *Principal Component Analysis in Meteorology*, pp. 199–205, Elsevier Sci., New York, 1988.

Rajagopalan, B., Y. Kushnir, and Y. M. Tourre, Observed decadal midlatitude and tropical Atlantic climate variability, *Geophys. Res. Lett.*, *21*, 3967–3970, 1998.

Robertson, A. W., C. R. Mechoso, and Y. J. Kim, The influence of Atlantic sea surface temperature anomalies on the North Atlantic oscillation, *J. Clim.*, *13*, 122–138, 2000.

Ruiz-Barradas, A., J. A. Carton, and S. Nigam, Structure of interannual-to-decadal climate variability in the tropical Atlantic sector, *J. Clim.*, *13*, 3285–3297, 2000.

Saravanan, R., and P. Chang, Interaction between tropical Atlantic variability and El Niño–Southern Oscillation, *J. Clim.*, *13*, 2177–2194, 2000.

Seager, R., Y. Kushnir, M. Visbeck, N. Naik, J. A. Miller, G. Krahmann, and H. M. Cullen, Causes of Atlantic Ocean climate variability between 1958 and 1998, *J. Clim.*, *13*, 2845–2862, 2000.

Servain, J., I. Wainer, J. P. McCreary, and A. Dessier, Relationship between the equatorial and meridional modes of climatic variability in the tropical Atlantic, *Geophys. Res. Lett.*, *26*, 485–488, 1999.

Sutton, R. T., S. P. Jewson, and D. P. Rowell, The elements of climate variability in the tropical Atlantic region, *J. Clim.*, *13*, 3261–3284, 2000.

Tomas, R. A., and P. J. Webster, The role of inertial instability in determining the location and strength of near-equatorial convection, *Q. J. R. Meteorol. Soc.*, *123*, 1445–1482, 1997.

Tomas, R. A., J. R. Holton, and P. J. Webster, The influence of cross-equatorial pressure gradients on the location of near-equatorial convection, *Q. J. R. Meteorol. Soc.*, *125*, 1107–1127, 1999.

Uvo, C. B., C. A. Repelli, S. E. Zebiak, and Y. Kushnir, The relationship between tropical Pacific and Atlantic SST and northeast Brazil monthly precipitation, *J. Clim.*, *11*, 551–562, 1997.

Wagner, R. G., and A. M. Da Silva, Surface conditions associated with anomalous rainfall in the Guinea coastal region, *Int. J. Climatol.*, *14*, 179–199, 1994.

Waliser, D. E., and C. Gautier, A satellite-derived climatology of the ITCZ, *J. Clim.*, *6*, 2162–2174, 1993.

Wallace, J. M., Effect of deep convection on the regulation of tropical sea surface temperature, *Nature*, *357*, 230–231, 1992.

Wang, B., and Y. Wang, Dynamics of the ITCZ-Equatorial Cold Tongue Complex and causes of the latitudinal climate asymmetry, *J. Clim.*, *12*, 1830–1847, 1999.

Xie, P., and P. A. Arkin, Global Precipitation: A 17-year monthly analysis based on gauge observations, satellite estimates, and numerical model outputs, *Bull. Am. Meteorol. Soc.*, *78*, 2539–2558, 1997.

Xie, S.-P., and Y. Tanimoto, A pan-Atlantic decadal climate oscillation, *Geophys. Res. Lett.*, *25*, 2185–2188, 1998.

Xie, S.-P., Y. Tanimoto, H. Noguchi, and T. Matsuno, How and why climate variability differs between the tropical Atlantic and Pacific, *Geophys. Res. Lett.*, *26*, 1609–1612, 1999.

Yulaeva, E., and J. M. Wallace, The signature of ENSO in global temperature and precipitation fields derived from the microwave sounding unit, *J. Clim.*, *7*, 1719–1736, 1994.

Zebiak, S. E., Air-sea interaction in the equatorial Atlantic region, *J. Clim.*, *6*, 1567–1586, 1993.

————————

J. C. H. Chiang, Joint Institute for the Study of the Atmosphere and the Ocean, University of Washington, Box 354235, Seattle, WA 98195-4235, USA. (jchiang@atmos.washington.edu)

A. Giannini, National Center for Atmospheric Research, Advanced Study Program, Boulder, CO 80307, USA. (alesall@ucar.edu)

Y. Kushnir, Lamont-Doherty Earth Observatory, Columbia University, Route 9W, Palisades, NY 10964, USA. (kushnir@ldeo.columbia.edu)